

الجمهورية الجزائرية الديمقراطية الشعبية
PEOPLE'S DEMOCRATIC REPUBLIC OF ALGERIA
وزارة التعليم العالي والبحث العلمي
MINISTRY OF HIGHER SUPERIOR EDUCATION AND SCIENTIFIC RESEARCH
جامعة عمار تلجي بالأغواط
UNIVERSITY AMAR TELIDJI LAGHOUAT



كلية العلوم
FACULTY OF SCIENCES
Department OF Material Sciences

Master thesis

Domain : Material Sciences
Field : Physics
Option : Material physics
by:

Horimek Cherifa

thesis

physical properties of full and half Heusler alloys Co₂CrAl and CoCrSb ,First principal study .

Publicly defended before the jury consisting of:

Mr. FARES Faid	M.C.A	President
Mr. ELHAMRA Fatima	M.C.B	Examiner
Mr. GUEDDOUH Ahmed	M.A.A	Supervisor
Mr. BELKHIR Mohamed lamine	Doctor	co- Supervisor

2021/2022

Dedication

I dedicate this modest work to:

➤ *The dearest people in my life my parents (hadj Abdelkarim et taibaoui Z), Brothers (M.N.H.Y), and Sister (R .Z.A). and grandmothers (ben graina A et taibaoui H) and grandfathers (horimek mailoud et taibaoui ohmaimide).*

** Allah yahfadhoun ! **

➤ *Aunts (O, R, k, N, H, KH, V, A). and uncles (L, H, A, F, LA, k, M).*

➤ *My whole family without exception (Horimek and taibaoui).*

➤ *My teacher Gueddouh Ahmed and Dr lamine belkhir.*

➤ *All teachers of UNIVERSITE AMAR TELIDJI- LAGHOUAT.*

➤ *All my teachers that I consider them as my parents.*

➤ *All my friends (A.I.M.W.ch) and colleagues (Z.S.N.B.K.F....) without exception .*

➤ *Everything that encourages me and wishes me success.*

Horimek cherifa



Acknowledgments

I thank my god at all times. Allah. Which gave me hope and the energy to finish this modest work.

*I would like to express my deep respect and gratitude to **Dr. Geddouh. Ahmed**, Lecturer at Amer TELIDJI University, who gave me supervised and to guide me during the elaboration of this work, I thank her warmly for his precious advice, his availability and his qualities Human, and **lamine mohmed belkhir.**, Dr student, Laghouat, for their direction and follow-up this travail. and also I thank **Dr. safai Djamel**, Lecturer at Amer Telidji University because encourage me and wishe me success.*

*Likewise, I address my thanks to **Sir faid fars**, lecturer. at The University Amer Telidji, Laghouat, who did me the honour of agreeing to chair the jury of the dissertation. I would like to warmly thank **M^{elle}. ELHAMRA Fatima**, lecturer at Amer Telidji University, Laghouat, who are part of the jury and for spending their precious time examining my work.*

Finally, these thanks would not be complete without mentioning all my family and my friends who, through their encouragement and their moral assistance, enabled me to write this dissertation in the right conditions.



HORIMEK CHERIFA

List of tables

Table of Contents

<i>Dedication</i>	
<i>Acknowledgments</i>	<i>II</i>
<i>Table of Contents</i>	<i>III</i>
<i>List of Figures</i>	<i>V</i>
<i>List of tables</i>	<i>VI</i>
<i>General introduction</i>	<i>I</i>

Chapter I : Half and full of Heusler

I.1	Introduction	6
I.2	Origins of magnetic moments	6
➤	Orbital magnetic moment.....	7
➤	Spin magnetic moment.....	7
I.2.1	The different forms of magnetism	7
I.2.2	Curie temperature.....	9
I.2.3	half-metallic Materials	9
I.3	General information about Heusler alloys	10
I.3.1	Types of Heusler	11
I.3.2	Magnetism and Heusler alloys.....	15
I.3.3	Spintronics and applications.....	16

Chapter II : Theoretical framework

II	Theoretical framework	20
----	-----------------------------	----

II.1	Introduction	20
II.2	The basics of the theory	20
II.3	Resolution of the Schrödinger equation	21
II.3.1	Approximation de Born-Oppenheimer	21
II.4	Density functional theory (FTD).....	21
II.4.1	Kohn-Sham equations.....	23
II.4.2	Exchange and correlation function.....	24
II.4.2.2	Generalized gradient approximation (GGA)	25
II.5	The plane wave base	25
II.6	Calculation code : CASTEP	26

Chapter III : Results and discussion

III.1	Introduction	29
III.2	Computational Details.....	29
III.3	Convergence study	30
III.4	Physical and chemical	30
III.4.1	Structural properties.....	30
III.4.2	Energies Stabilities.....	33
III.4.3	Electronic Properties	34
III.4.4	Magnetic properties	39
III.4.5	Elastic Properties	41
III.4.6	Thermodynamic properties	47
	Conclusion Genirale.....	52

List of tables

Table	Title	Page
Chapter I		
1	Main characteristics of the different magnetic materials.	07
2	The different types of magnetic behavior	08
3	Different types of occupations of non-equivalent sites in the structure of type C1b.	12
4	Number, nature and distance of the first neighbors of each type of atoms in a full-Heusler X_2YZ alloy of structure L21. A is the lattice parameter of the alloy.	13
5	Three different types of atomic arrangement of $XX'YZ$ compounds.	15
Chapitre III		
1	The Convergence test of as a function of E_{cut} and k points for Co_2CrAl and $CoCrSb$	30
2	Lattice parameter a (Bohr), lattice volume, Total energy (eV) of Co_2CrAl alloys.	31
3	The Wyckoff positions of the three atoms, X, Y, and Z: $4a = (0, 0, 0)$ a, $4b = (0.5, 0.5, 0.5)$ a and $4c = (0.75, 0.75, 0.75)$ a..	32
4	the types of structures $CoCrSb$ alloys.	32
5	cohesive energy E_{coh} and formation energy E_f of Co_2CrAl alloy	33
6	gap energy for Co_2CrAl	35
7	gap energy for $CoCrSb$.	38
8	Total and partial magnetic moment of Co_2CrAl .	40
9	The calculated spin magnetic moments for $CoCrSb$ compounds for the three possible structural phases comparing with available data.	41
10	gives the calculated value of elastic property for Co_2CrAl	42
11	gives the calculated value of elastic property for $CoCrSb$	42
12	gives the calculated values of the Mechanical properties for Co_2CrAl	45
13	gives the calculated values of the Mechanical properties for $CoCrSb$	45
14	Groups together the results of calculation of thermodynamic parameters for the compound Co_2CrAl studied in this chapter.	48
15	Groups together the results of calculation of thermodynamic parameters for the compound $CoCrSb$ studied in this chapter.	48

List of figures

Figure	Title	Page
Chapter I		
1	Origins of magnetic moments	06
2	Classification of magnetic materials	09
3	spin polarization of Materials	10
4	Periodic table of elements	11
5	Overview of the different aspects of Heusler compounds from T. Graf and all	11
6	Crystal structure of half-Heusler XYZ alloys.	12
7	Inverse and regular structure of Mn ₂ -based Heusler compounds	14
8	Schematic illustration of the three possible non-equivalent structures of quaternary Heusler compounds (a) type 1, (b) type 2 and (c) type 3.	15
9	(Color online) Calculated total spin moment per unit cell as a function of the total number Z _t of valence electrons per unit cell for all the studied half (left panel) and full (right panel) Heusler alloys. The dashed line represents then Slater-Pauling behaviour.	16
Chapter II		
1	Diagram describing the iterative process for solving the Kohn-Sham equations	24
2	Comparison of a wave function in the coulomb potential of the nucleus to the one in the pseudopotential. The real and the pseudo-wave function and potential match above a certain cut off radius	26
Chapter III		
1	Crystal structures of the Compound Heusler Co ₂ CrAl: Full-Heusler regular (Structure of type AlCu ₂ Mn).	31
2	The optimized crystal structure of CoCrSb.	32
3	band Structure of Co ₂ CrAl	34
4	Total and partial density of state of Co ₂ CrAl	36
5	Band structures for CoCrSb (a) majority-spin and (b) minority-spin. The Fermi level is indicated by the dashed horizontal line	37
6	Calculated total spin density of states (DOS) of Type- II CoCrSb alloy	39
7	Anisotropy of Young's modulus and bulk's modules in Co ₂ CrAl and CoCrSb	47

General Introduction

General Introduction

Spin electronics or spintronic is a field of nanoscience which was born with the discovery of giant magnetoresistance (GMR) by Fert and Grünberg[1]. It is a technique, which unlike conventional electronics, exploits the spin degree of freedom of electrons in order to store information. The starting point of this new discipline of condensed matter physics is the experimental demonstration of spin-dependent electrical transport in Fe/Cr multilayers.

The classes of materials, who are used in the applications of this field (spintronic), are named: Heusler alloys, which were reported by Friedrich Heusler far back 1903[2] and since then, this continues to attract active research interests owing to their unique multifunctional properties and suitability spintronic, optoelectric, thermoelectric, magnetic shapememory applications[3].

Heusler alloys have been found to exhibit half-metallic character by the calculation results in the sense that the material is metallic in the spin up channel and semiconductor in the spin down direction, also, there is a complete spin polarization ($P=100\%$) of the conduction electrons at the Fermi level position.

In this work ferromagnetism and other related properties in Co-based Heusler alloys (Full and Half) have been investigated theoretically, by ab initio approach, based on the density functional theory (DFT), implemented in CASTEP code[4]. The Perdew-Burke-Ernzerhof parametrization of the generalized gradient approximation (PBE-GGA) [5] was used to account for the exchange–correlation energies in all the calculations. Using first-principles calculations, several properties as: structural, electronic, magnetic, elastic and thermodynamics, were investigated for Cobalt-based Heusler alloys (Co_2CrAl , CoCrSb), as results of properties calculations, the full Co_2CrAl and half CoCrSb Heusler alloys features are characterized by full spin polarization at the Fermi level, they exhibit a half metallicity and they have an integer number for magnetic moment, that they obey to Slater Pauling rules[6],[7].

General Introduction

This memoire is divided into three Chapters : is Chapter 1, where we present the description of Heusler alloys, Chapter 2 is dedicated to the basic concepts of density functional theory (DFT) and introduced the concept and formalism of calculations used at the present work. Chapter 3 presents the results of our calculations for Full and half Heusler alloys in this study (Co_2CrAl and CoCrSb). we close my memoire , with a general conclusion .

REFERENCES

- [1] M. N. Baibich *et al.*, « Giant magnetoresistance of (001) Fe/(001) Cr magnetic superlattices », *Phys. Rev. Lett.*, vol. 61, n° 21, p. 2472, 1988.
- [2] F. Heusler, « Über magnetische manganlegierungen », *Verhandlungen Dtsch. Phys. Ges.*, vol. 5, p. 219, 1903.
- [3] D. Kieven, R. Klenk, S. Naghavi, C. Felser, et T. Gruhn, « I-II-V half-Heusler compounds for optoelectronics: Ab initio calculations », *Phys. Rev. B*, vol. 81, n° 7, p. 075208, 2010.
- [4] M. Segall *et al.*, « First-principles simulation: ideas, illustrations and the CASTEP code », *J. Phys. Condens. Matter*, vol. 14, n° 11, p. 2717, 2002.
- [5] J. P. Perdew, « In Electronic Structure of Solids' 91; Ziesche, P.; Eschrig, H., Eds ». Akademie Verlag: Berlin, 1991.
- [6] J. C. Slater, « Wave functions in a periodic potential », *Phys. Rev.*, vol. 51, n° 10, p. 846, 1937.
- [7] L. Pauling, « The nature of the interatomic forces in metals », *Phys. Rev.*, vol. 54, n° 11, p. 899, 1938.

Chapter I

I.1 Introduction

Since the dawn of time and over the ages, magnetism has always fascinated minds. Considered one of the great miracles of nature. Research in these areas does not cease to develop until this day when magnetic materials are found everywhere in our daily lives, they are presented almost in all machines, starting from the simplest device which is Compass to the most complex devices such as computers.

Therefore, magnetism represents a set of physical phenomena in which objects exert attractive or repulsive forces on other materials. The electric currents and magnetic moments of the fundamental elementary particles are at the origin of the magnetic field that generates these forces. All materials are influenced, in a more or less complex way, by the presence of a magnetic field.

In the first part of this chapter, we will recall the important notions about the physics of spintronics to emphasize the interest and motivation of the subject. First of all, we will briefly address the different forms of magnetism (diamagnetism, paramagnetism, ferromagnetism, anti-ferromagnetism and ferrimagnetism).and finally General information about Heusler alloys.

I.2 Origins of magnetic moments

Two sources are at the origin of the magnetic moment in an atom:

- ❖ **Orbital magnetic moment.**
- ❖ **Spin magnetic moment.**

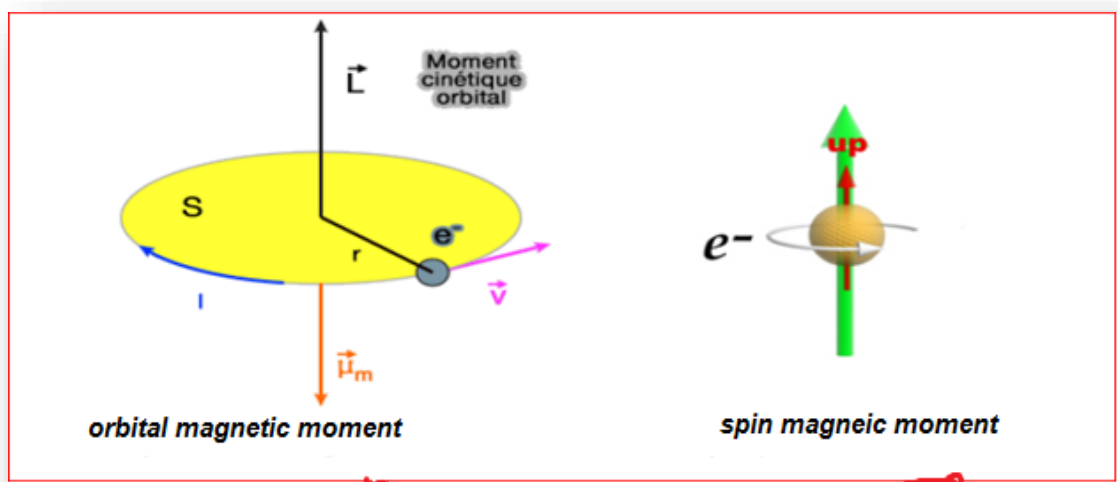


Figure 1: Origins of magnetic moments

➤ Orbital magnetic moment

The movement of electrons in the atom creates current loops. The magnetic moment associated with these orbital movements enters for a part in the magnetic moment of an atom but it is not enough to account for all the magnetization.

$$\vec{\mu}_l = -\frac{\mu_B}{\hbar} \vec{I} \quad (I.1)$$

Where $\mu_B = 9.274 \times 10^{-24} A.m^2$ is the Bohr magneton, this equation means that the electron is assimilated to an infinitesimal current loop whose orbital kinetic moment is Quantified

➤ Spin magnetic moment

$$\vec{\mu}_s = -g \frac{\mu_B}{\hbar} \vec{S} \quad (I.2)$$

Where $g \approx 2$ is pure number, called Landé factor (1921). This number varies depending on the nature of the particle.

I.2.1 The different forms of magnetism

The magnetic state of matter depends on:

- The nature of each atom:
 - Magnetic i.e. electrons in the outer layer not paired.
 - Non-magnetic i.e. the electrons appear.
- The nature and the electrons of the neighboring atoms and the inter atomic distances.
 - The interactions between them (the exchange "spin" and the coulombic "charge").
- The arrangements of the magnetic spins of atoms and their values (random, parallel and antiparallel).
- The temperature and applied magnetic field.

Table. 1. Main characteristics of the different magnetic materials

Material type	Susceptibility	χ as a function of temperature	Examples
Diamagnetic	$\cong -10^{-6}$	Independent	Cu, Ag, Au, organic molecule
Paramagnetic	$\cong +10^{-3}$	$\chi = C/T$ (Curie's law)	Na, Cr (TN=35°C), Mn (-173 °C), Al, Mo, Ti, Zr
Ferromagnetic	Very large and positive	$\chi \rightarrow +\infty$	Fe (Tc=770°C),

			Co ($T_C = 1131\text{ °C}$), Ni ($T_C = 358\text{ °C}$)
Ferrimagnetic	large and positive	$\chi \rightarrow +\infty$	Fe ₂ O ₃
Antimagnetic	Small and positive	$\chi \propto 1/T$	NiO ($T_N = 257\text{ °C}$), MnO ($T_N = -151\text{ °C}$)

With: C: is the Curie constant and T_C is the Curie temperature

At present, the different categories of magnetic materials are presented:

Table. 2: The different types of magnetic behavior

Type	Comportement	Arrangement
<i>Diamagnétique</i>	<ul style="list-style-type: none"> ✓ Non magnétique ✓ Pas d'interaction ✓ Lorsqu'on applique un champ H, on obtient un moment magnétique opposé au H. 	
<i>Paramagnétique</i>	<ul style="list-style-type: none"> ✓ Magnétique ✓ Les moments désordonnés dans toutes les directions ✓ Pas d'interaction ✓ Lorsqu'on applique un champ H, on obtient $M_{tot} \neq 0$ 	
<i>Ferromagnétique</i>	<ul style="list-style-type: none"> ✓ Magnétique ✓ Ordonnés parallèlement ✓ Existe une interaction ✓ Distance plus (AFM) ✓ Moment résultant non nul $M_{tot} \neq 0$ même pour $H=0$ 	
<i>Antiferromagnétique</i>	<ul style="list-style-type: none"> ✓ Magnétique $M_{tot} = 0$ ✓ Ordonnés antiparallèlement ✓ Existe une interaction ✓ Distance suffisamment petites 	
<i>Ferrimagnétique</i>	<ul style="list-style-type: none"> ✓ Atomes magnétiques ayant des M différents $M_{tot} \neq 0$ ✓ Ordonnés antiparallèlement ✓ Existe une interaction. ✓ Distances suffisamment petites. 	

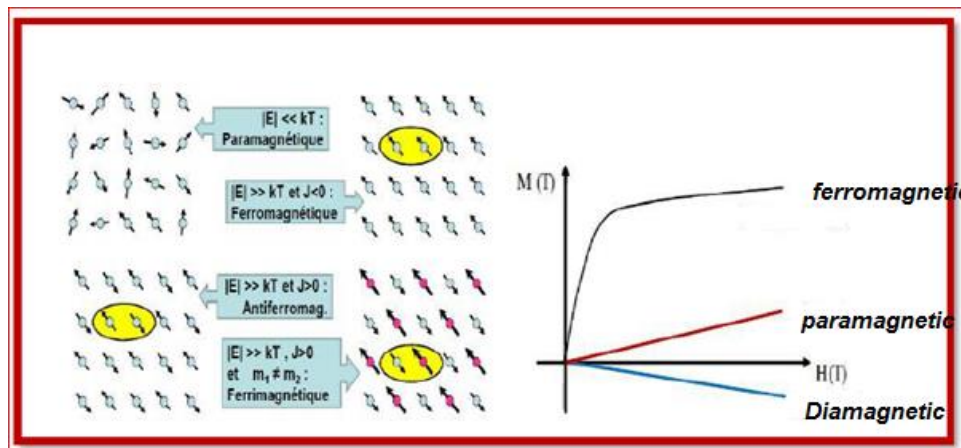


Figure 2: Classification of magnetic materials[1].

I.2.2 Curie temperature

The Curie temperature (or Curie point) of a ferromagnetic or antiferromagnetic material is the temperature T_C at which the material loses its permanent magnetization. The material then becomes paramagnetic. This phenomenon was discovered by the French physicist Pierre Curie in 1895. Permanent magnetization is caused by the alignment of magnetic moments. The magnetic susceptibility above the Curie temperature can then be calculated from the Curie-Weiss law, which derives from Curie's law. By analogy, the Curie temperature of a ferroelectric material is also called the temperature at which the material loses its permanent polarization. This temperature is usually marked by a maximum of the dielectric constant.

I.2.3 half-metallic Materials

The first appearance of the term "half metal" was in the early 1980s [2]. In a half-metal, according to Groot, only electrons of a given spin orientation ("up" or "down") are metallic, while electrons of the other spin orientation have a semiconductor behavior. In other words, half metals have spin polarization. 100% since the contribution of electrons around the Fermi level exists in a single spin direction (up or down).

$$P = \frac{N_{\uparrow}(E_F) - N_{\downarrow}(E_F)}{N_{\uparrow}(E_F) + N_{\downarrow}(E_F)} \times 100$$

(I.3)

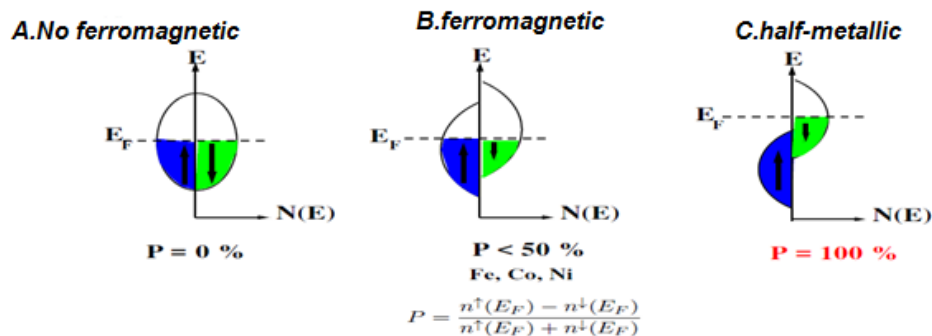


Figure 3: Spin polarization of Materials.

It is observed that for a half-metallic material the Fermi level passes through a gap of energy for one direction of spin and by a band of energy for the other direction.

Half metals should not be confused with strong ferromagnetic such as Co or Ni. Indeed, the 3d bands of the Co or Ni are well polarized in spin at 100% but the 4s.c is why no material consisting of a single atom is half-metallic. The 4s bands, which are at Fermi, are not polarized. Electrons "up " or "down» are therefore present at Fermi. To obtain a half-metal, it is then necessary a hybridization of the 3d and 4s bands so that the Fermi level is no longer in the half-metal band should also not be confused with semi-metals, such as bismuth, which have an equal number of holes and electrons due to a slight overlap between the valence and conduction bands.

I.3 General information about Heusler alloys

Since the discovery of the ferromagnetic half-metallicity of Heusler alloys, these the latter have become an area of research interest for spin electronics [3].

The heusler compounds are magnetic intermetallics with a crystalline cubic structure with centered faces and a composition of XYZ (half-Heuslers) or X₂YZ (Full-Heuslers), where X and Y are transition metals and Z is in the p block. The term Heusler alloys is attributed to a group of compounds that contain about 3000 identified compounds. These remarkable compounds were first discovered by Fritz Heusler in 1903 discovered that an alloy with a formula of the type Cu₂MnAl behaves like a ferromagnetic material.

The main combinations of Heusler alloys are presented in

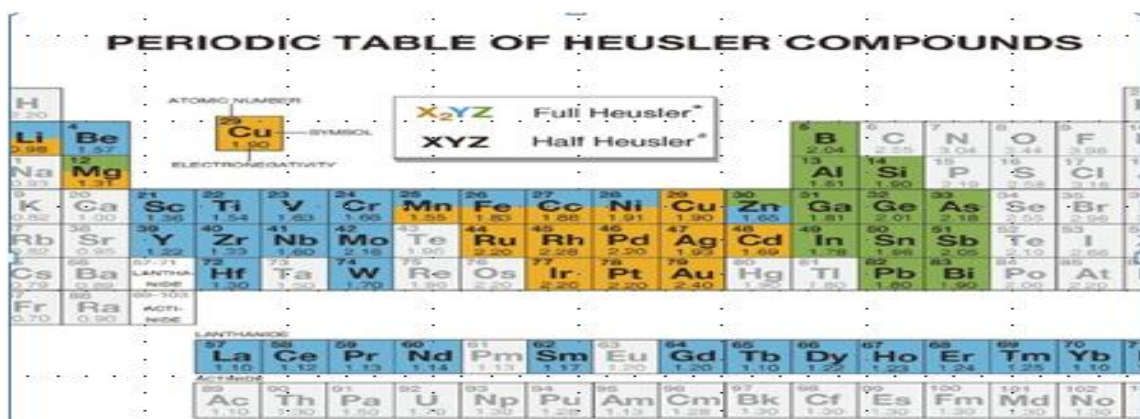


Figure 4: Periodic table of elements [1]

The name of Heusler alloys has been generalized to encompass two classes of materials: Half-Heusler with the general formula XYZ and Full-Heusler alloys with X₂YZ. The X and Y are elements of the transition metal group, when the Z component comes from the elements of the III-V group. The main combinations of Heusler alloys are shown in the Figure 4. The

Figure 5. summarizes all the important aspects concerning these exceptional materials, ranging from semiconductors, metals and magnets to topological isolators with many technological applications in spintronics, thermoelectrics, optoelectronics [4]:



Figure. 5: Overview of the different aspects of Heusler compounds from T. Graf and all [5].

I.3.1 Types of Heusler

✓ The half-Heusler

The half-Heuslers crystallize in a non-Centro-symmetric cubic structure (partial groups $N^{\circ}216$, $F^{-}43m$, $C1b$) which can be derived from the tetrahedral structure of the ZnS type by a filling of the octahedral sites of the lattice. This type of half-Heusler structure can be characterized by the interpenetration of three face-centered cubic sublattices, each of which is occupied by the X, Y and Z atoms[6]. The occupied positions are 4a (0, 0, 0), 4b (1/2, 1/2, 1/2), and 4c (1/4, 1/4, 1/4). This structure corresponds to that of a full-Heusler alloy X_2YZ where every second X atom would have been removed from the elementary lattice (Figure I-3). In principle, three non-equivalent atomic arrangements are possible in this type of structure (Table I-2). In the half-Heusler structure; one finds different types of atomic disorder.

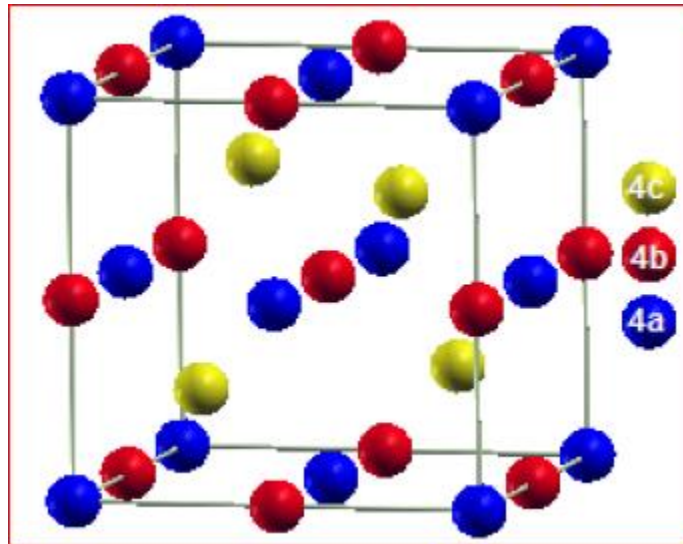


Figure 6: Crystal structure of half-Heusler XYZ alloys.

Table. I.3: Different types of occupations of non-equivalent sites in the structure of type C1b.

	4a	4b	4c
I	X	Y	Z
II	Z	Z	Y
III	Y	X	X

✓ Full-Heusler alloys (X_2YZ)

Complete Heusler alloys are ternary intermetallic compounds that can be defined by the stoichiometric formula X_2YZ , where X and Y are transition elements and Z is a group III, IV or V element. Cu_2MnSn was the first Heusler alloy discovered by Heusler. Subsequently, a large number of Heusler alloys were discovered with a wide range of physical properties.

Table I.4: Number, nature and distance of the first neighbors of each type of atoms in a full-Heusler X_2YZ alloy of structure L21. A is the mesh parameter of the alloy.

Atome	1 ^{er} voisins	d/a_0	2 ^e voisins	d/a_0	3 ^e voisins	d/a_0
X	4Y et 4Z	0.433	6X	0.5	12X	0.707
Y	8X	0.433	6Z	0.5	12Y	0.707
Z	8X	0.433	6Y	0.5	12Z	0.707

Which consists of two parts:

✚ Full Heusler regular

X_2YZ type Heusler or full-Heusler alloys that crystallize in the cubic space group $Fm\bar{3}m$ (No. 225) with Cu_2MnAl (L21) as the prototype. The X atoms occupy position 8c (1/4, 1/4, 1/4), the Y atoms and Z atoms are located at positions 4a (1/2, 1/2, 1/2) and 4b (0,0, 0), respectively. This structure consists of four interpenetrating cfc sub lattices, two are occupied by the X atom. A rock salt structure is formed by the least and most electropositive elements (Y and Z atoms). Due to the ionic character of their interaction, these elements have octahedral coordinates. On the other hand, all the tetrahedral sites are occupied by the X atom. This structure can also be considered as a zinc blende.

✚ Full Heusle inverse

The inverse Heusler structure is observed, if the atomic number of Y is higher than that of X of the same period ($Z(Y) > Z(X)$), but it can also appear in transition metal compounds of different periods. Heusler inverses have cubic space group $F\bar{3}m$ (No. 216) with Hg_2MnAl (XA) as prototype, in all cases the element X is more electropositive than Y. Therefore, X and Z form a rock salt structure to achieve octahedral coordination for X. The remaining X and Y atoms occupy the tetrahedral sites with fourth-order symmetry. The structure is still described by four interpenetrating cfc sub lattices, but the X atoms do not form a simple cubic lattice. Instead, they are placed on positions 4a (1/2,1/2, 1/2) and 4d (3/4, 3/4, 3/4), while the Y and Z atoms are located at 4b (1/4, 1/4, 1/4) and 4c(0, 0, 0), respectively. This inverse Heusler structure is often observed for Mn₂-based materials with $Z(y) > Z(Mn)$.

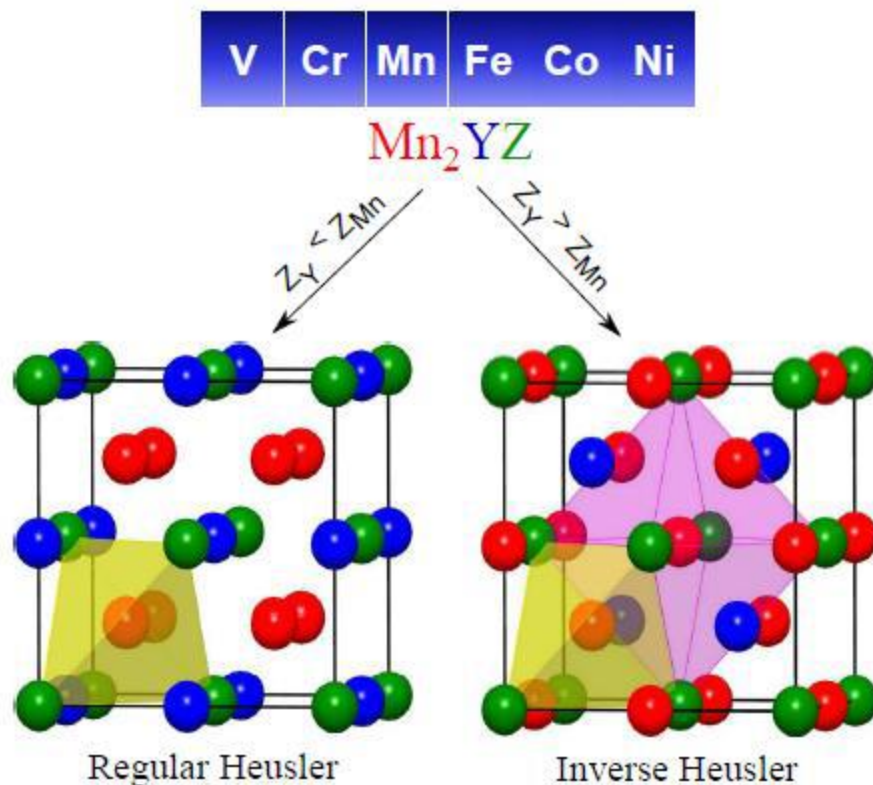


Figure 7: Inverse and regular structure of Mn_2 -based Heusler compounds

Both inverse and regular structures can be formed for Mn_2 -based Heusler compounds depending on the atomic number of the element at the Y position.

✓ **Quaternary Heusler alloys:**

Another family of LiMgPdSn-type Heuslers, also known as the compounds LiMgPdSb [7] type Heusler compounds called quaternary Heuslers. These are compounds quaternary compounds of chemical formula $(XX')YZ$ where X, X', and Y are atoms of transition metals. The valence of X' is lower than the valence of X, and the valence of the element Y is lower than the valence of both X and X'. The sequence of atoms along the diagonal of the cube (CFC) is X-Y-X'-Z which is energetically the most stable [8].

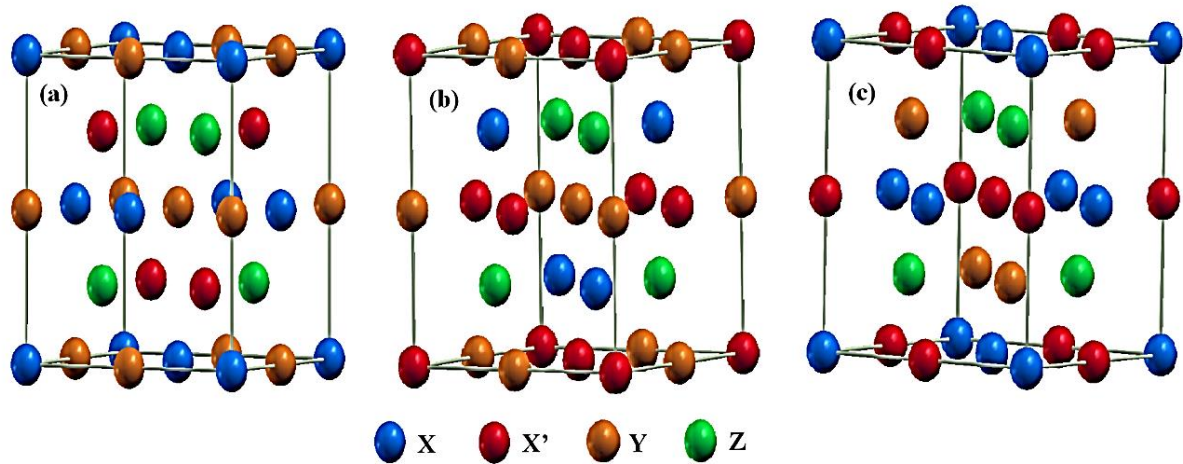


Figure 8: Schematic illustration of the three possible non-equivalent structures of quaternary Heusler compounds (a) type 1, (b) type 2 and (c) type 3.

Tab.I.5. Three different types of atomic arrangement of $XX'YZ$ compounds:

structure	X	X'	Y	Z
Type 1	4a (0, 0, 0)	4c (1/2, 1/2, 1/2)	4b(1/4, 1/4, 1/4)	4d(3/4, 3/4, 3/4)
Type 2	4b(1/4, 1/4, 1/4)	4c (1/2, 1/2, 1/2)	4a (0, 0, 0)	4d(3/4, 3/4, 3/4)
Type 3	4a (0, 0, 0)	4b(1/4, 1/4, 1/4)	4c (1/2, 1/2, 1/2)	4d(3/4, 3/4, 3/4)

I.3.2 Magnetism and Heusler alloys

Solids are bound in a crystal by the attractive electrostatic interaction between the charges of electrons and protons in the nuclei. There are contributions to this mechanism by magnetic forces. These, however, are very small. Solids can be separated into classes according to their physical properties. The differences between the types of solids in general are caused by the ion nuclei and the outermost electrons of an atom. Metals, semiconductors, insulators and semi-metals are classes of materials essentially divided by the fact that their electronic structures facilitate electrical conduction.

✓ Slater-Pauling's behavior

Heusler alloys are also intermetallic compounds based on transition metals and they have rather a localized magnetism compared to a route character. The explanation of the origin of the magnetism of these alloys is very complicated but their magnetic moments vary according to the number of valence electrons (N_v) and the crystal structure. This behavior is called Slater-Pauling[7], [9].

The total moment of full Heusler alloys (half metal) can be estimated by the simple rule

$M_t = Z_t - 24$. Also the total moment of half Heusler alloys (half metal) can be estimated by the simple rule $M_t = Z_t - 18$.

Since: Z_t is the total number of valence electrons, its value is sum of the number of spin-up and spin-down electrons:

$$Z_t = N_{\uparrow} + N_{\downarrow} \quad (I.4)$$

While the moment total μ_t is as follows:

$$\mu_{tot} = N_{\uparrow} - N_{\downarrow} \quad (I.5)$$

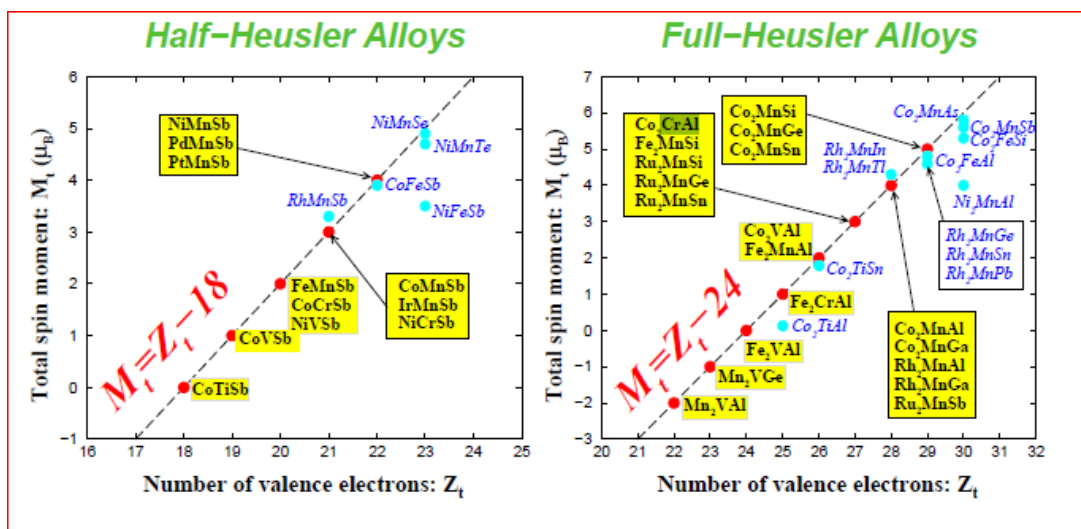


Figure 9 : (Color online) Calculated total spin moment per unit cell as a function of the total number Z_t of valence electrons per unit cell for all the studied half (left panel) and full (right panel) Heusler alloys. The dashed line represents then Slater-Pauling behaviour.

I.3.3 Spintronics and applications

behaving like an antenna..Spintronics In recent years, spintronics, or spin electronics, has become a key technology in the field of information storage. It is a new technology that takes advantage of the electron's spin and more precisely of that, the phenomenon of spin-polarized current.

✓ Applications of Spintronics

✚ Magnetoresistance (MR)

Magnetoresistance (MR) The general idea of spin electronics is based on the passage of electron current in ferromagnetic materials and to use the influence of spin on the mobility of electrons in these materials. Since the discovery of the giant magnetoresistance (GMR) by Fert and Grünberg [10], [11] in 1988, this field has developed around three major challenges:

increasing the magnetoresistance rate, spin injection from a ferromagnetic material to a semiconductor material and the spin transfer phenomenon. Magnetoresistance (MR) is a main effect in spintronics, which concerns the variation of the electrical resistance of a conductor under the application of a magnetic field. Today, very high MR values are highly sought after for the development of spintronic devices such as magnetic memories (MRAM). There are several types of MR but the most used are the GMR and the tunnel magnetoresistance (TMR).

✚ Giant magnetoresistance GMR

Giant magnetoresistance was discovered in monocrystalline layers in 1988 by two independent teams: that of Albert Fert, from the University of Paris Sud-Orsay, and the one led by Peter Grünberg of the Jülich Research Centre (North Rhine-North Rhine- Westphalia, Germany). On 9 October 2007, Albert Fert and Peter Grünberg received jointly the Nobel Prize in Physics for their discovery.

GMR is a quantum effect observed in thin film structures composed of a alternation of layers of ferromagnetic and non-magnetic layers. It manifests in the form of a significant decrease in resistance observed under application an external magnetic field. There is an antiferromagnetic coupling between magnetizations of two successive ferromagnetic layers through the non-ferromagnetic layer magnetic. This coupling tends to align the magnetizations of the ferromagnetic layers successive antiparallel in zero magnetic field. When a magnetic field is applied, the magnetizations rotate in the direction of the field until they become parallel to the saturation field.

✚ tunneling magnetoresistance TMR

TMR tunneling magnetoresistance was discovered in 1975 by Michel Jullière, a professor at INSA Rennes, using iron as a ferromagnetic material and Germanium as an insulator. It is a property that appears when two ferromagnetic materials are separated by a thin insulating membrane of the order of 1nm.

The electrical resistance to the passage of current by tunneling from one material to another through the insulating layer varies according to the relative orientation of the two magnetic layers. This resistance usually reaches its maximum in an antiparallel alignment. The effect could only be achieved at room temperature from 1995 thanks to the work of Jagadeesh Moodera after the growing interest in the field motivated by the discovery of GMR. This effect today is the basis of MRAM (Magnetic Random Access Memory)[12] and hard drive sensors.

REFERENCES

- [1] A. Hirohata *et al.*, « Heusler alloy/semiconductor hybrid structures », *Curr. Opin. Solid State Mater. Sci.*, vol. 10, n° 2, p. 93-107, 2006.
- [2] G. A. Prinz, « Spin-polarized transport. », *Phys. Today*, vol. 48, n° 4, p. 58-63, 1995.
- [3] R. A. De Groot, F. M. Mueller, P. G. Van Engen, et K. H. J. Buschow, « New class of materials: half-metallic ferromagnets », *Phys. Rev. Lett.*, vol. 50, n° 25, p. 2024, 1983.
- [4] T. Graf, C. Felser, et S. S. Parkin, « Simple rules for the understanding of Heusler compounds », *Prog. Solid State Chem.*, vol. 39, n° 1, p. 1-50, 2011.
- [5] T. Graf, F. Casper, J. Winterlik, B. Balke, G. H. Fecher, et C. Felser, « Crystal structure of new Heusler compounds », *Z. Für Anorg. Allg. Chem.*, vol. 635, n° 6-7, p. 976-981, 2009.
- [6] P. Webster, « Magnetic and chemical order in Heusler alloys containing cobalt and manganese », *J. Phys. Chem. Solids*, vol. 32, n° 6, p. 1221-1231, 1971.
- [7] J. C. Slater, « The ferromagnetism of nickel », *Phys. Rev.*, vol. 49, n° 7, p. 537, 1936.
- [8] V. Alijani, J. Winterlik, G. H. Fecher, S. S. Naghavi, et C. Felser, « Quaternary half-metallic Heusler ferromagnets for spintronics applications », *Phys. Rev. B*, vol. 83, n° 18, p. 184428, 2011.
- [9] L. Pauling, « The nature of the interatomic forces in metals », *Phys. Rev.*, vol. 54, n° 11, p. 899, 1938.
- [10] M. N. Baibich *et al.*, « Giant magnetoresistance of (001) Fe/(001) Cr magnetic superlattices », *Phys. Rev. Lett.*, vol. 61, n° 21, p. 2472, 1988.
- [11] G. Binasch, P. Grünberg, F. Saurenbach, et W. Zinn, « Enhanced magnetoresistance in layered magnetic structures with antiferromagnetic interlayer exchange », *Phys. Rev. B*, vol. 39, n° 7, p. 4828, 1989.
- [12] S. D. Sarma, « Spintronics: A new class of device based on electron spin, rather than on charge, may yield the next generation of microelectronics », *Am. Sci.*, vol. 89, n° 6, p. 516-523, 2001.

Chapter II

II.1 Introduction

Numerical simulation has acquired a prominent place in the physical sciences. It can assist the experiment. It makes it possible to explore the physical properties of matter with tolerable precisions. Among the numerical methods, elected in the field of materials science, is the ab initio calculation or first principle. These methods seek to predict the properties of materials, based on the equations of quantum mechanics.

This second chapter serves to describe the foundations of ab- initio calculus and particularly DFT (Density Functional Theory) is a Method most used in quantum calculations of the electronic structure of matter (atoms, molecules, solids) both in condensed matter physics and quantum chemistry.

In this chapter we will try to follow with the reader the path of the different approaches leading to formulation and implementation (DFT).

II.2 The basics of the theory

For a solid body consisting of a large number of interacting electrons and nuclei. The equation that describes physical properties (energy, electronics, optics ...) of this quantum system in its fundamental state is the Schrödinger equation, independent of time, written as follows [1].

$$H\psi = E\psi \quad (II.1)$$

Where,

H: represents the Hamiltonian.

Ψ : represents the wave function describing the state of the system.

E: the total energy of the system.

Represents the total Hamiltonian operator of the system given by the following relation:

$$H = T_e + T_N + V_{n-n} + V_{n-e} + V_{e-e} \quad (II.2)$$

The Hamiltonian terms of the system are:

$$\triangleright T_e = -\sum_i^n \frac{\hbar^2}{2m_e} \nabla_i^2 \quad : \text{Total kinetic energy of electrons.}$$

$$\triangleright T_N = -\sum_I^N \frac{\hbar^2}{2M_I} \nabla_I^2 \quad : \text{Total kinetic energy of nuclei.}$$

- $V_{n-n} = \sum_{I=1}^N \sum_{J>I}^N \frac{e^2}{4\pi\epsilon_0} \frac{Z_I Z_J}{|R_I - R_J|}$: Potential energy between nuclei.
- $V_{n-e} = - \sum_{i=1}^n \sum_{I=1}^N \frac{e^2}{4\pi\epsilon_0} \frac{Z_I}{|r_i - R_I|}$: Potential energy nuclei and electrons.
- $V_{e-e} = \sum_{i=1}^n \sum_{j>i}^n \frac{e^2}{4\pi\epsilon_0} \frac{1}{|r_i - r_j|}$: Interaction energy between electrons.

The solution of equation (II.1) of an N body is analytically impossible, for this several approximations have been developed in order to be able to solve this equation.

II.3 Resolution of the Schrödinger equation

II.3.1 Approximation de Born-Oppenheimer

In 1927, the first level of approximation to simplify the resolution of the equation (II.3) is the Born-Oppenheimer approximation [2] by separating the electronic part from the nuclear part in the wave function ψ this is why it is called adiabatic [3] which is based on the large difference in mass between electrons and nuclei[4].

The electronic Hamiltonian is written:

$$\mathbf{H}_e = \mathbf{T}_e + \mathbf{V}_{N-e} + \mathbf{V}_e \quad (\text{II.3})$$

The solution of the Schrödinger equation with this Hamiltonian is given by:

$$H_e \psi_e = E_e \psi_e \quad (\text{II.4})$$

The total energy of the system will therefore be the sum of the electronic energy and the energy of the nuclei:

$$E_{tot} = E_e + E_{noy} \quad (\text{II.5})$$

This approximation does not give real energy, so physicists have developed other methods of approach to give more precision.

II.4 Density functional theory (DFT)

One of the most widely used ab initio methods is density functional theory. Density Functional Theory (which will be called in French La théorie de la fonctionnelle de la densité (DFT))[5],[6],[7],[4] is a reformulation of the N-body quantum problem into a problem dealing solely with electron density. Today, DFT is one of the most widely used methods for quantum calculations of the electronic structure of the solid, because the reduction of the

problem it brings makes it possible to make it possible to calculate the ground state of a system with a large number of electrons.

The theory of the density functional is based on two theorems stated by Hohenberg and Kohn in 1964:

➤ Hohenberg and Kohn's theorems

The basic formalism of the DFT is based on the Hohenberg-Kohn theorem (1964)[5].

This approach is based on two theorems

➤ The first theorem

This theorem highlights a unique correspondence between the outer potential $V_{ext}(r)$ and the electron density $n(r)$. Since it fixes the number of electrons, it then also uniquely determines the wave function and thus the electronic properties of the system.

For a given system, the energy will therefore be written as follows:

$$E[n(r)] = T[n(r)] + V_{e-e}[n(r)] + V_{ext}[n(r)] \quad (II.6)$$

Or:

$$E[n(r)] = F_{HK}[n(r)] + \int V_{ext}(r)n(r)dr \quad (II.7)$$

With $F_{HK}[n(r)] = T_e[n(r)] + V_{e-e}[n(r)]$ which is the Hohenberg-Kohn functional containing kinetic energy and potential energy due to the electron-electron repulsive interaction.

➤ The second théorème

The second theorem postulates that energy, functional of electron density, obeys the variational principle but applied this time to a functional of electron density

$$E[n_0] = \min E[n] \quad (II.8)$$

n_0 : Being the density of the ground state [8].

II.4.1 Kohn-Sham equations

In 1965 Kohn and Sham (KS) [9] proposed a practical method for using density functional theory. The Kohn and Sham process leads to a set of mono electronic Schrödinger equations known as Kohn-Sham equations.

They introduced an additional development that consists of replacing the interactive real system into a non-interactive fictitious system whose ground state is characterized at all points by the same density as the interacting electron system.

So the Kohn-Sham equation can be written:

$$\left(-\frac{\nabla_i^2}{2} + V_{eff}(r) \right) \varphi_i(r) = \varepsilon_i \varphi_i(r) \quad , i = 1, \dots, n \quad (II.9)$$

Where the actual potential is defined by:

$$V_{eff}(r) = V_{ext}[n(r)] + \int \frac{n(r')}{|r-r'|} dr' + V_{xc}[n(r)] \quad (II.10)$$

With $V_H[n(r)] = \int \frac{n(r')}{|r-r'|} dr'$ is the Hartree potential of electrons

The exchange potential and correlation is given by the derived functional:

$$V_{xc}[n(r)] = \frac{\partial E_{xc}[n(r)]}{\partial n(r)} \quad (II.11)$$

And the density is given by a sum on all the occupied orbitals:

$$n(r) = \sum_i^N |\varphi_i(r)|^2 \quad (II.12)$$

So the actual potential can be written:

$$V_{eff}(r) = V_{ext}[n(r)] + \int \frac{n(r')}{|r-r'|} dr' + V_{xc}[n(r)] \quad (II.13)$$

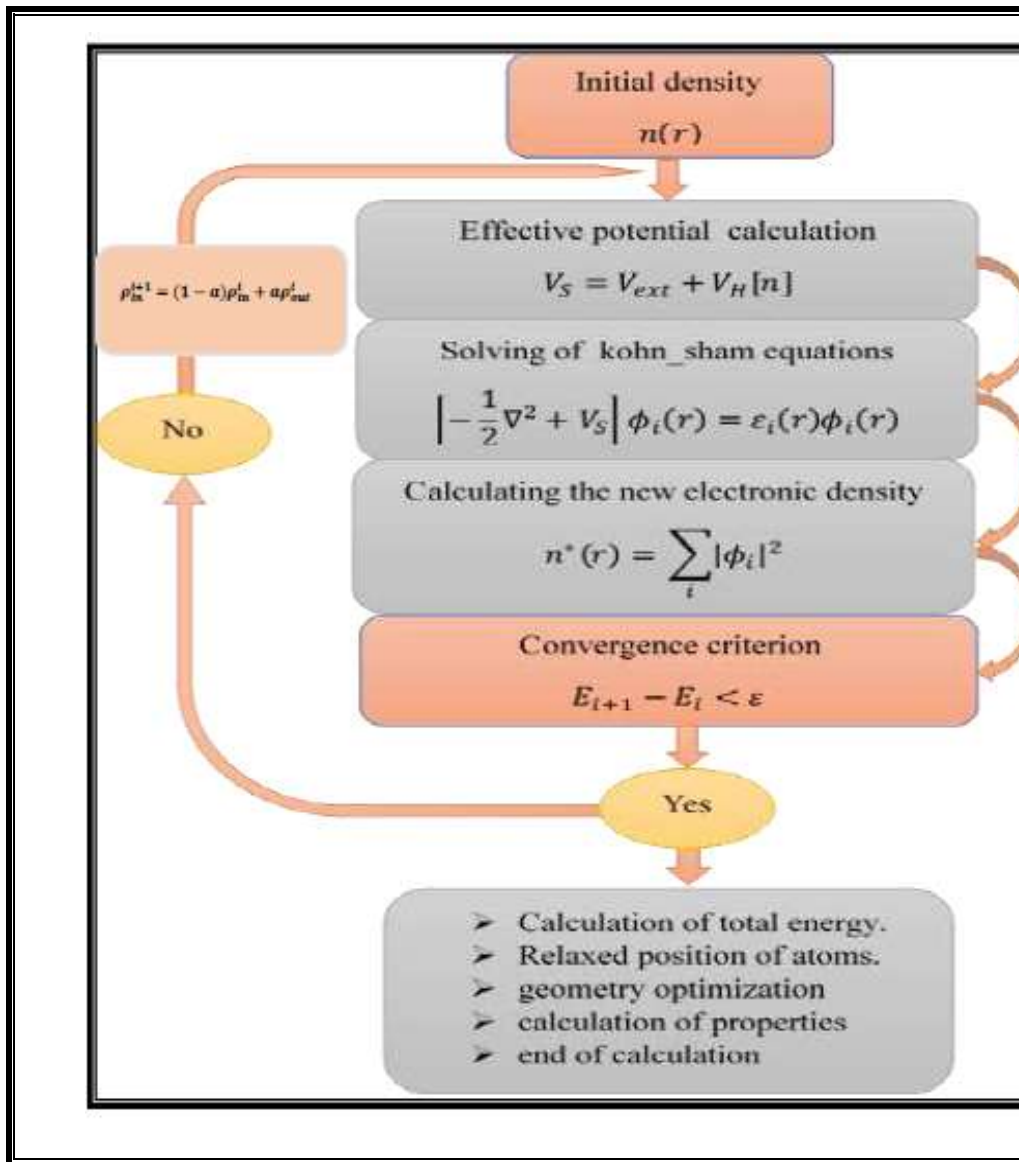


Figure 1: Diagram describing the iterative process for solving the Kohn-Sham equations[5]

II.4.1.1 Exchange and correlation function

The exchange and correlation functional in the Kohn and Sham equations is only possible by giving an analytic form to the exchange and correlation energy. The most commonly used approximations:

- Local density approximation (LDA)
- Generalized gradient approximation (GGA) and derived methods based on a non-local approach.

II.4.1.2 Generalized gradient approximation (GGA)

Generalized gradient approximation was introduced to improve the accuracy of LDA results. It consists in writing the exchange and correlation energy not only as a function of the electron density $\rho(\mathbf{r})$ but also of its gradient.

$$E_{xc}^{GGA}[n(\mathbf{r}), \nabla n(\mathbf{r})] = \int n(\mathbf{r}) \varepsilon_{xc}^{GGA}[n(\mathbf{r}), \nabla n(\mathbf{r})] d\mathbf{r} \quad (II.14)$$

$\varepsilon_{xc}^{GGA}[n(\mathbf{r}), \nabla n(\mathbf{r})]$: The exchange-correlation energy per electron in a mutually interacting electron system of non-uniform density.

II.5 The plane wave base

Plane wave bases, associated with periodic boundary conditions, are often suitable for the study of solids insofar as they satisfy Bloch's theorem by construction. Plane wave decomposition of wave functions consists of expressing these wave functions using Fourier series:

$$\varphi_j^k(\mathbf{r}) = \Omega^{-1/2} \sum_G C_j^k(\mathbf{G}) e^{i(\mathbf{k}+\mathbf{G})\cdot\mathbf{r}} \quad (II.15)$$

But in practice:
$$\frac{\hbar^2}{2m} |\mathbf{K} + \mathbf{G}| < E_{cut} \quad (II.16)$$

Where:

E_{cut} : Cut-off energy.

E_{cut} : Kinetic energy less than.

➤ Pseudopotential method

The pseudopotential method is based on the assumption that only valence electrons (the outermost electrons) contribute significantly to the physical and chemical properties of a given electronic system. The valence electrons are the only ones involved in the chemical bonding picture, whereas the core electrons (the most internal electrons) are not strongly sensitive to the chemical environment. Ionic cores (nuclei and core electrons) are thus considered to be "frozen" in their atomic configurations; it is the approximation of the frozen heart [10]. So, this method is to deal explicitly only with the valence electrons, which then move in an effective potential, produced by these inert ionic cores, called **pseudopotential**.

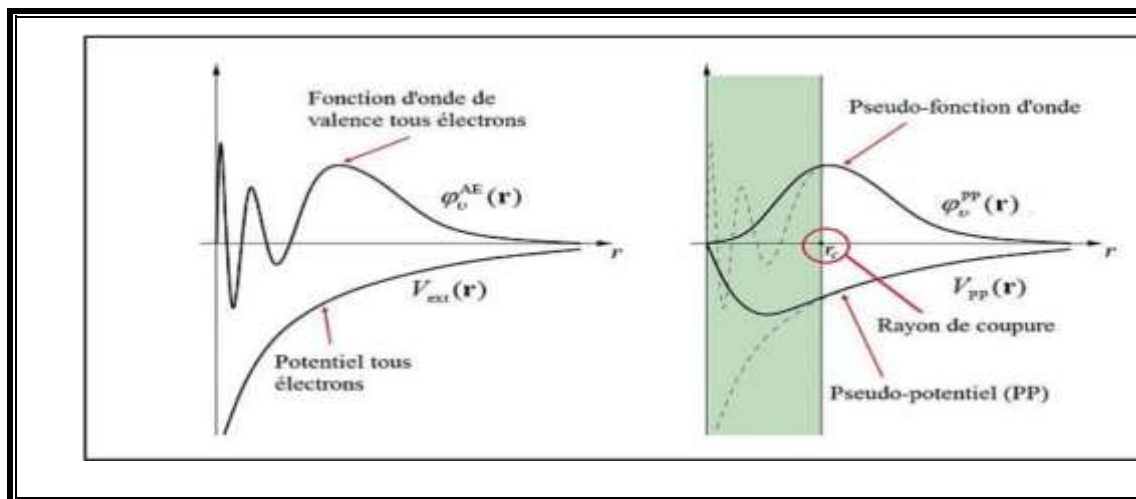


Figure **Erreur ! Il n'y a pas de texte répondant à ce style dans ce document..1:** Comparison of a wave function in the coulomb potential of the nucleus to the one in the pseudopotential. The real and the pseudo-wave function and potential match above a certain cutoff radius[11].

II.6 Calculation code : CASTEP

The Cambridge Serial Total Energy Package Software (CASTEP) code[1] is a simulation program widely used in solid state physics. It is an abinitio calculation code and is part of a set of numerical simulation software called Materials Studio (MS) and marketed by Dassault Systèmes Biovia ©. CASTEP is developed in the Condensed Matter Theory group at the University of Cambridge, UK, it is a program that uses density functional theory (FTD) to simulate the properties of solids, and can predict properties, including elastic constants, structural properties, energy band diagrams, electron state densities, charge densities and optical properties, as well as vibrational and thermodynamic properties.

CASTEP works on Windows and other windows. A graphical interface compliant with Microsoft Windows standards, allows the user to interact with 3D graphics models, configure calculations and analyze the results through simple dialog boxes familiar to any Windows user.

REFERENCE

- [1] M. Segall *et al.*, « First-principles simulation: ideas, illustrations and the CASTEP code », *J. Phys. Condens. Matter*, vol. 14, n° 11, p. 2717, 2002.
- [2] M. Born et J. R. Oppenheimer, « On the quantum theory of molecules », *Сборник Статей К Мультимедийному Электронному Учебно-Методическому Комплексу По Дисциплине «физика Атома И Атомных Явлений» от Ред Шундалов МБ БГУ Физический Факультет*, 1927.
- [3] H. Chen, Z. Wei, H. He, X. Zheng, K. Wong, et S. Yang, « Solvent Engineering Boosts the Efficiency of Paintable Carbon-Based Perovskite Solar Cells to Beyond 14% », 2016, doi: 10.1002/aenm.201502087.
- [4] W. Kohn, « Nobel Lecture: Electronic structure of matter—wave functions and density functionals », *Rev. Mod. Phys.*, vol. 71, n° 5, p. 1253, 1999.
- [5] P. Hohenberg et W. Kohn, « Inhomogeneous electron gas », *Phys. Rev.*, vol. 136, n° 3B, p. B864, 1964.
- [6] E. Engel, S. Keller, et R. Dreizler, « Generalized gradient approximation for the relativistic exchange-only energy functional », *Phys. Rev. A*, vol. 53, n° 3, p. 1367, 1996.
- [7] R. G. Parr, « W. Yang Density functional theory of atoms and molecules », *Oxf. Univ. Press*, vol. 1, p. 1989, 1989.
- [8] L. KIROUANI, « Structure et organisation de la filière avicole en Algérie-Cas de la wilaya de Bejaia », *El-Bahith Rev. Univ. Mira Bejaia*, 2015.
- [9] W. Kohn et L. J. Sham, « Self-consistent equations including exchange and correlation effects », *Phys. Rev.*, vol. 140, n° 4A, p. A1133, 1965.
- [10] X.-Q. Chen, H. Niu, D. Li, et Y. Li, « Modeling hardness of polycrystalline materials and bulk metallic glasses », *Intermetallics*, vol. 19, n° 9, p. 1275-1281, 2011.
- [11] A. N. MAHAMMEDI, « ÉTUDE ab-initio DES DÉFAUTS INTRINSÈQUES DANS LES MATÉRIAUX CHALCOPYRITES Cu-III-S₂ », 2012.

Chapter III

II.1 Introduction

In this chapter, we present the results for the optimized structural parameters and the predicted elastic, electronic, magnetic, anisotropy, and thermodynamic properties for the cubic intermetallic compounds Full Heusler (Co_2CrSb) and Half Heusler (CoCrSb).

II.2 Computational Details

All calculations conducted in the present work were performed using CASTEP code [1] based on the pseudo-potential [2] and plane waves schemes (PP-PW) of DFT theory. We make use of Generalized Gradient Approximation (GGA) as parameterized by Perdew-Burk Ernzerh of "PBE". Electron-ionic interactions were treated by on-the-fly generated ultra-soft pseudo-potentials (OTFG-USPP) [2]. Valence states were modeled by ($3d^7 4s^2$) for Co, ($3s^2 3p^6 3d^5 4s^1$) for Cr, ($1s^2 2s^2 2p^6 3s^2 3p^1$) for Al, and ($4d^{10} 5s^2 5p^3$) for Sb.

In a DFT calculation, the physical properties of a system are functional of the electron density of the ground state. This density is the one that minimizes the total energy of the system. It is therefore imperative to express this energy with the greatest possible precision.

Firstly, we start to verify whether the selected calculation parameters reproduce the experimental ground state geometry. The bulk Co_2CrAl , CoCrSb structures were used for the subsequent tight optimizations. The total energy was minimized self consistently using the Broyden-Fletcher- Goldfarb-Shanno algorithm (BFGS) [3-7].

Both lattice parameters and atomic positions were fully relaxed, respecting the following convergence criteria:

- ❖ Tolerance in energy: $5 \cdot 10^{-6}$ (eV/atom).
- ❖ Max force: 0.001 (eV/Å°).
- ❖ Max stress: 0.002 GPa.
- ❖ Max displacement: $5 \cdot 10^{-4}$ (Å°).

II.3 Convergence study

Before exposing our results, I first study the parameters that crucially condition all ab-initio simulations in DFT + pseudo potentials formalism. In general, there are two adjustments to be made which are: The size of the plane wave basis by the choice of the cut off E_c (cut off energy) which allows a correct approximation of the eigen functions, and the quality of the sampling of the Brillion zone (by the number of points k).

For Co_2CrAl and also CoCrSb , The convergence test for the two studied compounds, allow us to choose as calculation parameters the values:

Table 1: The Convergence test of as a function of E_{cut} and k points for Co_2CrAl and CoCrSb .

	cut off	K points
Co_2CrAl	600eV	$10 \times 10 \times 10$
CoCrSb	600eV	$10 \times 10 \times 10$

The choice of these settings can be used to optimize the accuracy based on available computing resources.

II.4 Physical properties

II.4.1 Structural properties

This part of this work is devoted to the study of the structural properties of our compounds: Co_2CrAl and CoCrSb . This kind of study is of major interest, because it allows to collecting information on the microscopic structure of materials and will thus have a relatively important impact on the prediction of other properties.

➤ Full Heusler

To determine the equilibrium lattice parameter and find out how the total energy varies according to this parameter, we performed structural optimizations on the Full Heusler Co_2CrAl alloy for type of AlCu_2Mn (L21, space group Fm-3m, N°225) where the atom Al occupies 4a (0,0,0) , the atoms Cr at 4c (0.5, 0.5,0.5) and Co are located 4d (0.25, 0.25,0.25) and 4b (0.75, 0.75,0.75), (See Figure 1).

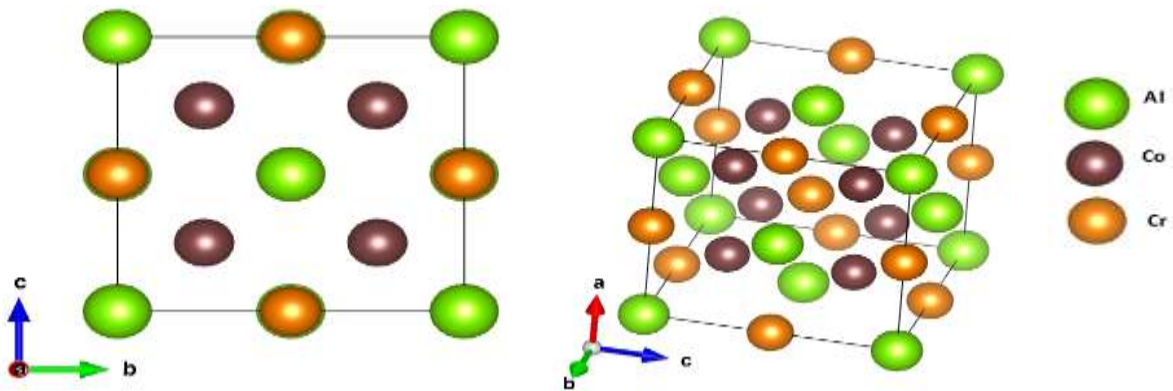


Figure 1: Crystal structures of the Compound Heusler Co_2CrAl : Full-Heusler regular (Structure of type AlCu_2Mn).

The obtained results including the ground state equilibrium structural parameters, atomic Coordinates, cell volumes of our materials are represented in **Tables 2**.

Table 2: lattice parameter a (Bohr), lattice volume, Total energy (eV) of Co_2CrAl alloys.

Co ₂ CrAl		
Space group, Z Symmetry	L21, space group Fm-3m, Cubic Our cal	N°225) other cal
Unit cell parameters (Å)	5.71	5.72 ^a , 5.74 ^f , 5.75 ^h
Cell volume (Å ³)	186.18	187.14,
Energy(eV)	- 4711.710	-

^a Ref.[8], ^fRef.[9], ^hRef[10]

It can be deduced from the table that our results are in good agreement with those found in previous theoretical investigations.

➤ Half Heusler

We started by calculating the equilibrium lattice constant of the HH compound CoCrSb considering the three possible site arrangement of X and Y atoms shown in Figure 2. In Table 3, the Wyckoff [11] positions of the three atoms and vacancy are given based on in Type-I, Type-II, and Type-III phases which conform to $F\bar{4}3m$ space group.

The different types of structure studied:

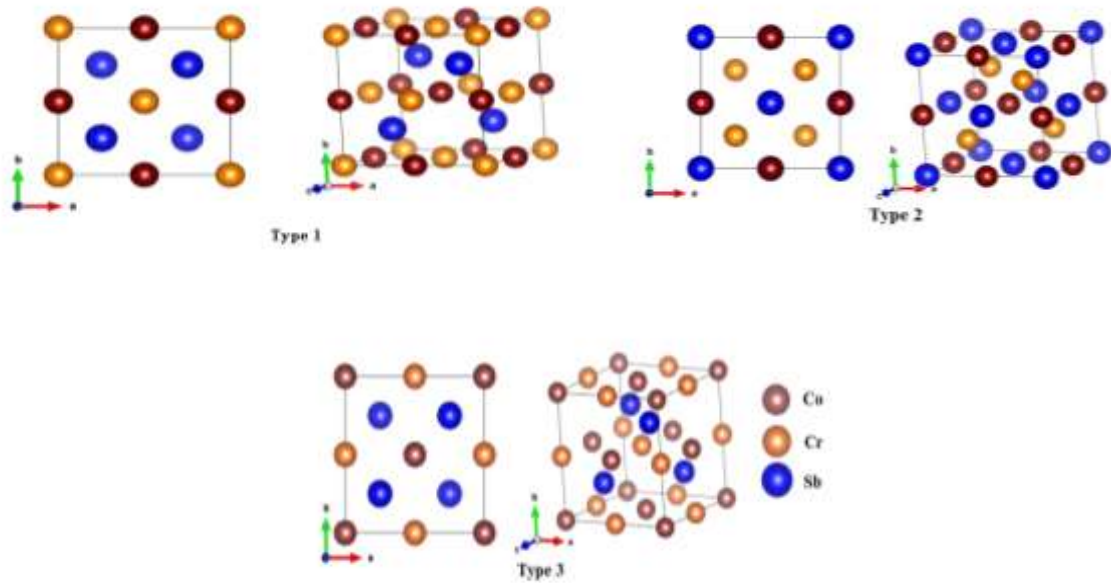


Figure 2: The optimized crystal structure of CoCrSb.

Table 3. The Wyckoff positions of the three atoms, X, Y, and Z: $4a = (0, 0, 0) a$, $4b = (0.5, 0.5, 0.5) a$ and $4c = (0.75, 0.75, 0.75) a$.

Structural Phase	X	Y	Z
Type 1	4b	4a	4c
Type 2	4c	4b	4a
Type 3	4a	4c	4b

Table 4: the types of structures CoCrSb alloys.

Alloys	Structural Phase	Calculations	a_0 (Å)	$V(\text{Å}^3)$	E_{min}
CoCrSb	Type 1	This Work	6.00	216	-5900.27
		other calculations	-	219.26	
	Type 2	This Work	5.84	199.18	-5901.34
		other calculations	5.82 b	199.18	
	Type 3	This Work	5.91	206.43	-5900.26
		Other calculations	5.93 d	208.53	

^bRef.[12]^dRef.[13],

The equilibrium lattice constant (a_0), the minimum energy (E_{\min}), and volume are reported in Table 4. The Type- II phase is the most stable structural phase (Figure 2 and Table 4). The lattice constants are smaller in this phase more significant than in other structural phases.

II.4.2 Energies Stabilities

➤ Formation and cohesive Energies

The cohesive energy (E_{coh}) of a material, (a useful fundamental property), is a measure of the relative binding forces. The stability of our compounds can be evaluated by calculating two energy parameters, cohesive energy E_{coh} and formation energy E_f defined as follows

$$E_{coh}(Co_2CrAl) = \frac{E_{total}(Co_2CrAl,Cell) - nE_{iso}(Co) - nE_{iso}(Cr) - nE_{iso}(Al)}{n} \quad \text{III. 1}$$

$$E_f(Co_2CrAl) = E_{coh}(Co_2CrAl) - E_{coh}(Co) - E_{coh}(Cr) - E_{coh}(Al) \quad \text{III. 2}$$

$$E_{coh}(CoCrSb) = \frac{E_{total}(CoCrSb,Cell) - nE_{iso}(Co) - nE_{iso}(Cr) - nE_{iso}(Sb)}{n} \quad \text{III. 3}$$

$$E_f(CoCrSb) = E_{coh}(CoCrSb) - E_{coh}(Co) - E_{coh}(Cr) - E_{coh}(Sb) \quad \text{III. 4}$$

Table 5: cohesive energy E_{coh} and formation energy E_f of Co_2CrAl alloy

	$E_f(Co_2CrAl)(\text{mail})$	$E_{coh}(Co_2CrAl)(\text{mail})$
Co_2CrAl	-1.59 eV	-31.24 eV
$CrCoSb$	-65.55 eV	-76.11 eV

Where: $E_{coh}(Co_2CrAl)$ and $E_{coh}(CoCrSb)$, are the cohesive energy of Co_2CrAl and $CoCrSb$, respectively, per unit formula; $E_f(Co_2CrAl)$ and $E_f(CoCrSb)$, are the formation energies; $E_{coh}(Co, Cr, Al, Sb)$ are the cohesive energy of element per atom; $E_{total}(Co_2CrAl, Cell)$ and $E_{total}(CoCrSb)$ are the total calculated energies of Co_2CrAl and $CoCrSb$; $E_{iso}(Co, Cr, Al, Sb)$ are the total energy of an isolated Co, Cr, Al, Sb atom and finally n refer to the number of unit formula.

Table 5 require negative values of $E_{coh}(Co_2CrAl)$, $E_{coh}(CoCrSb)$ and $E_f(Co_2CrAl)$, $E_f(CoCrSb)$ to refer to a **energetically** stable structure.

II.4.3 Electronic Properties

The analysis of the electronic structures of a compound makes it possible to precise nature of the bonds between the atoms constituting the solid. This analysis allows a good understanding of the different properties of the material at the macroscopic scale. Indeed, most physical properties are directly related to electronic properties. To characterize the electronic structure of a solid, we have complementary tools such as electronic state density (DOS) and band structure.

➤ Full Heusler

II.4.3.1 Band Structures

The band structure is a representation in the reciprocal space subjected to the dispersion relation, which helps us to better understand the phenomenon of half-metallicity in an alloy.

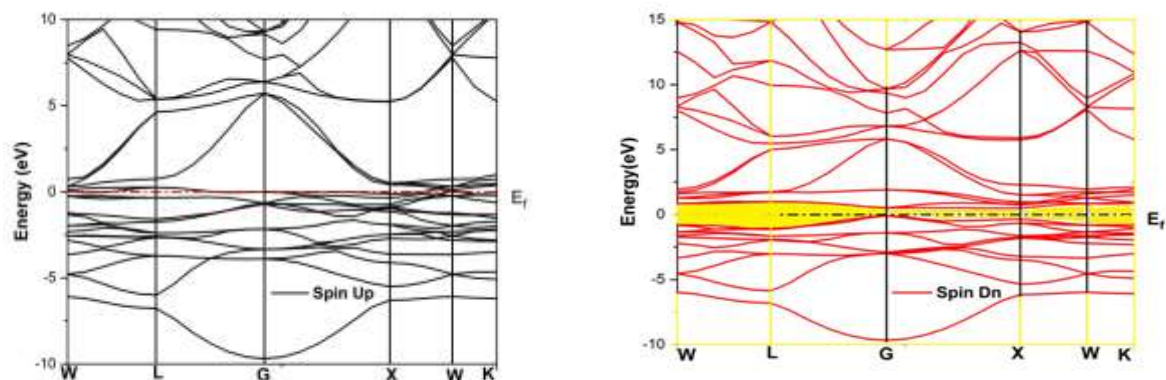


Figure 3 : Band Structure of Co_2CrAl .

It can be said that the Co_2CrAl material are semiconductors in the spin-dn state. And metal in the spin-up state. Then the most important remark is the presence of electronic state at the Fermi level in the band structure of the spin-up electrons.

This means that the system has a half-metallic character. The results obtained from the strip structure show a half-metallic behavior for the two spin projections.

The conduction band is located at the point X; it is thus an indirect gap. The value of the gap energy for Co_2CrAl

Table 6: gap energy for Co₂CrAl.

Alloys	Gap Energy (eV)	Our cal (eV)	othor cal (eV)
Co ₂ CrAl	$\Gamma \rightarrow X$	0.72	0.72 ^h , 0.75 ^E

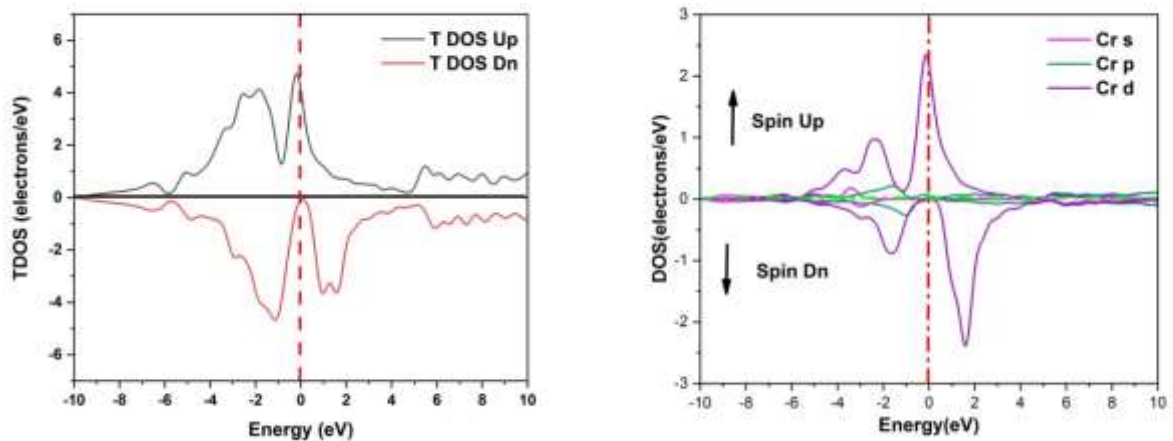
^hRef.[14], ^ERef.[15],

We believe it is important to point out that there are no experimental data on the gap of Co₂CrAl.

II.4.3.2 Density of states

State density (DOS) is an important physical quantity for understanding the physical properties of a material. Most transport properties are determined on the basis of knowledge of state density. It also makes it possible to know the nature of the chemical bonds in a material (by calculating the occupancy rate of each atomic state) and consequently, the charge transfer between atoms.

In an attempt to elucidate the nature of the electronic band structure, we also calculated the total and partial density of state, as shown in Figures 4. Most of the transport properties are determined based on the knowledge of the density of state.



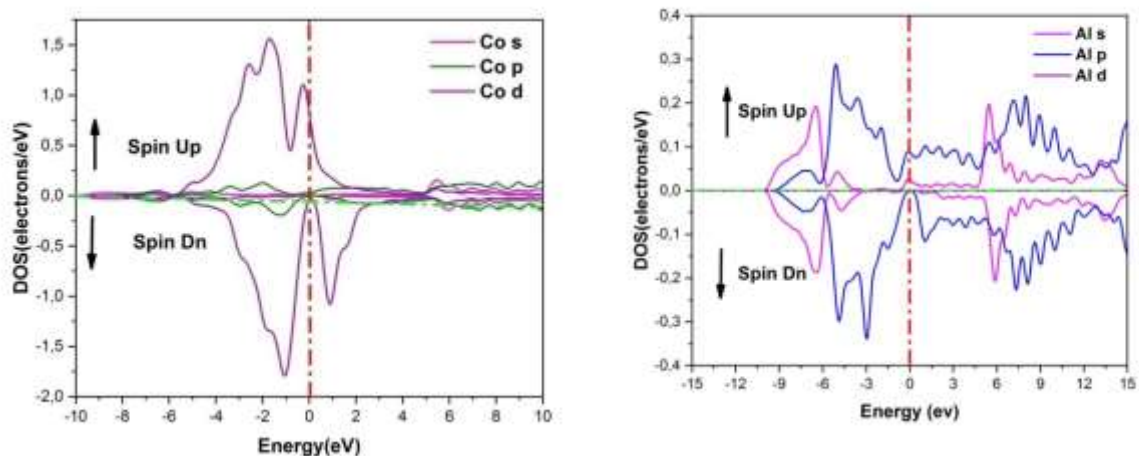


Figure 4: Total and partial density of state of Co_2CrAl

From figure 4, it is clear the existence of distinct region in spin-up state and in spin-down state for Co_2CrAl material there is distinct region separated by gap.

➤ In the spin-up state:

The first region is located from -12 eV to -7 eV below the Fermi level. This region is composed entirely of Al 's' states, above them, bands of Co 'd' states and located around -7 eV to -1.8 eV for Co_2CrAl material, the third region from -1.8 eV to 0eV, the band of The valence states are dominated by the Cr 'd' states for Co_2CrAl . The fourth region is located from 0 eV to 8 eV. The conduction band consists mainly of the 'd' orbital's of Cr and 'd' of Co Co_2CrAl .

➤ In the spin-down state:

The first region is located from -12 eV to -7 eV below the Fermi level. This region is composed entirely of 's' states of Al, above them, the band of 'd' states of Co and located around -7 eV to -0 eV for Co_2CrAl material, the third region from 0 eV to 9 eV: the conduction band is composed mainly of 'd' orbital's of Cr and 'd' of Co for Co_2CrAl . The Density of state confirms the metallic character for the majority spin and an absence of minority electronic state which brings us closer to the semiconductor character. This indicates a semi-metallic behavior for the two spin projections for Co_2CrAl .

The half-metallicity decreases from 100% for CoCrSb and further confirm half-metallicity for CoCrSb, as shown in Table 7.

Table 7: gap energy for CoCrSb.

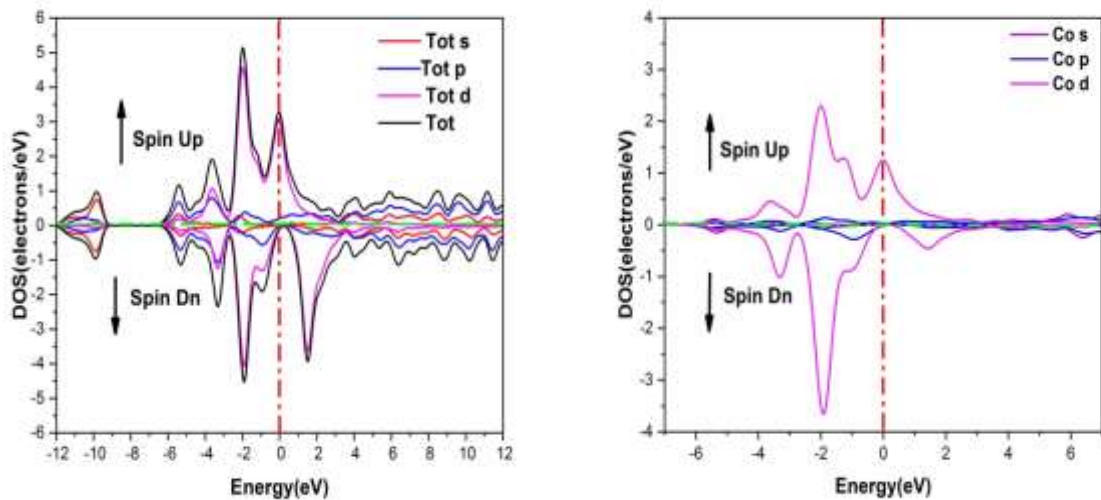
Composes	Gap energy (eV)	Our cal (eV)	Author-cal (eV)
CoCrSb	$\Gamma \rightarrow X$	0.77	0.77a

^a Ref.[17]

We believe it is important to point out that there are no experimental data on the gap of CoCrSb.

II.4.3.2 Density of states

Figure 6 displays the total DOS in which for the majority-spin (up spin) channel, the energy bands exhibit a metallic overlap with the EF for all the alloys, whereas in the minority-spin (down spin) direction, an energy gap is opened and the EF locates within the gap for CoCrSb, Hence, CoCrSb is half-metallic (with spin polarized of 100%),



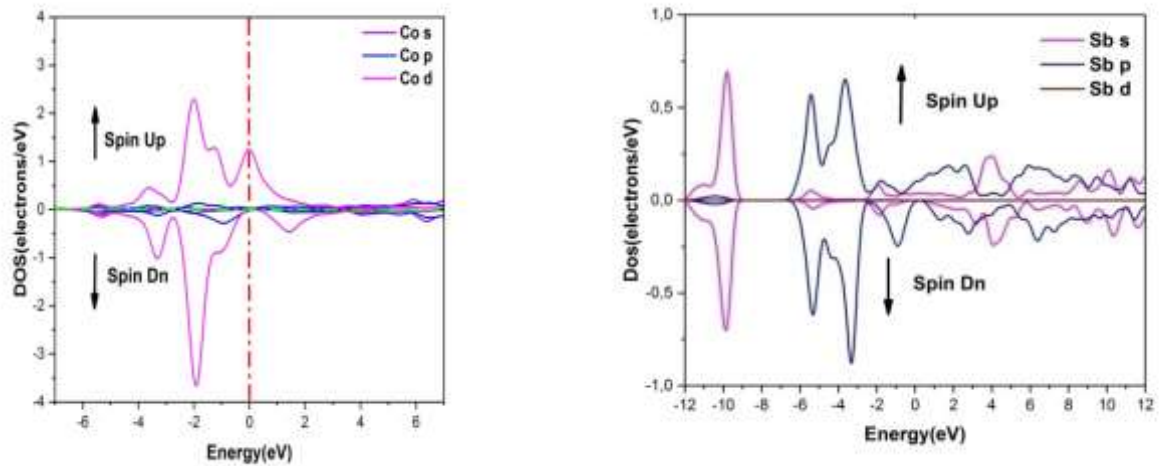


Figure 6: Calculated total spin density of states (DOS) of Type- II CoCrSb alloy.

II.4.4 Magnetic properties

The magnetic moment is represented by the spin magnetic moment defined by the total occupancy of the majority spin orbital's minus the total occupancy of the minority spin orbital's.

The energy band structure of a half metallic material exhibits an asymmetry between the spin up and spin down states with an energy gap or pseudo gap at the Fermi level. This gives rise to polarizations of the conduction electrons at the Fermi level that can reach 100%

The spin P polarization at EF is expressed in terms of the density of up-spin and down-spin states, $\rho \uparrow (EF)$ and $\rho \downarrow (EF)$ by the relation [18].

$$p = \frac{N(up) - N(dn)}{N(up) + N(dn)} \times 100 \quad \text{III. 5}$$

In half-metallic compounds, the spin moment per unit formula is an integer, Since the carried magnetic moment is equal to the difference between the number of spin up electrons and the number of spin down electron, an integer value of the carried magnetic moment is found.

➤ Full Heusler

Table 8: Total and partial magnetic moment of Co_2CrAl .

Moment Magnetic (μB)	Materiel : Co_2CrAl
Co	0.60
Cr	1.96
Al	0.60
Moment Total (μB)	3.00
Autre travaux théoriques (moment total (μB))	3.0110 _o
Spin Polarization %	100

Ref.[19]

The results in Table (8) show that the compound Co_2CrAl a total magnetic moment value of 3.00 μB . Our results are in good agreement with theoretical results.

The spin polarization is significant for compound Co_2CrAl , $P=100\%$.

The magnetic moment of our compound is $3\mu\text{B}$, satisfying the Slater-Pauling rule [20, 21]:

$$M_t = Z_t - 24 \quad \text{III. 6}$$

Z_t : is the total number of valence electrons:

$$Z_t = 27 \quad \text{III. 7}$$

$$M_t = 27 - 24 = 3\mu\text{B} \quad \text{III. 8}$$

Therefore, this compound is a demi-metallic material and obeys the (Slater-Pauling) rule.

The main contribution in the magnetic moment is due to the Cr atom, while an important contribution due to the Co atom is also noticed.

We can see that the values of the polarization are important. A polarization of 100% is characteristic of a half-metal.

It is important to underline that, to our knowledge; the scientific community does not have any experimental, so no experimental values of the magnetic moments for these materials.

➤ **Half Heusler**

Table 9. The calculated spin magnetic moments for CoCrSb compounds for the three possible structural phases comparing with available data.

Moment magnétique (μ_B)	Matériau : CoCrSb
Co	-0.79
Cr	3.09
Sb	-0.30
Moment Total (μ_B)	2.00
autres travaux théoriques (moment total (μ_B))	2.00a
Spin Polarization %	100

aRef.[22]

The calculated total and partial magnetic moments for all phases are listed in Table 9. It is seen that for CoCrSb, irrespective of the structural phase, the major contribution to the total magnetic moment comes from the Y (Cr) atom, CoCrSb, it is only in the Type II - phase that the major contributors to the magnetic moment come from the Y atom. As shown in Table 3, the total magnetic moments for CoCrSb are greater than 1, which indicates that these materials have ferromagnetic properties.

The magnetic moment of our compound is $2\mu_B$, satisfying the Slater-Pauling rule [20, 21]:

$$M_t = Z_t - 18 \quad \text{III. 9}$$

Z_t : is the total number of valence electrons:

$$Z_t = 20 \quad \text{III. 10}$$

$$M_t = 20 - 18 = 2\mu_B \quad \text{III. 11}$$

II.4.5 Elastic Properties

The elastic behavior of solids is related to the stiffness of the atomic bond. For example, if the type of bonding in a given solid is known, one can predict some aspects of its elastic behavior such as the modulus of elasticity. Conversely, one can use information about the elastic properties to understand the type of atomic bond. Cubic materials have three independent elastic constants namely C_{11} , C_{12} and C_{44} . The constants are evaluated by a total energy calculation for a perturbed system, using the Mehl model [23] which has been used successfully for several systems. The figure below illustrates the three types of mechanical constraints.

➤ **Full Heusler**

Table 10: gives the calculated value of elastic property for Co2CrAl

	Our calculation
C ₁₁	251.328
C ₁₂	171.3536
C ₄₄	147.16455

➤ **Half Heusler**

Table 11: gives the calculated value of elastic property for CoCrSb

	Our calculation
C ₁₁	190.52945
C ₁₂	74.3422
C ₄₄	55.549

The elastic constants are grouped in table 11 and 12. We did not find any experimental data on the elastic property of Co2CrAl and CoCrSb material's. The present results are then a predictive approach for this type of material. The mechanical stability of the crystals has been the subject of extensive theoretical studies. The systematic study of the stability of the lattice was made by Born and Huang [24] who formulated the stability criterion, it is expressed in terms of elasticity constants C_{ij} by

$$C_{11} + 2C_{12} > 0, C_{44} > 0, C_{11} > 0, C_{12} < B < C_{11}, C_{11} - C_{12} > 0 \quad \text{III. 12}$$

It is clear that the condition on the mechanical stability criteria is satisfied for the Co2CrAl material.

The determination of the elastic constants allows us to approach the mechanical properties of our materials such as the shear modulus, the Young's modulus and the Poisson's ratio.

✓ **Shear modulus**

In strength of materials, the shear modulus, also called the slip modulus, modulus, Coulomb modulus or second Lamé coefficient, is a physical quantity specific to each material and is used to characterize the deformations caused by shear forces. This modulus is given as a function of the elastic constants in the following form:

$$G_H = \frac{C_{11} - C_{12} + 3C_{44}}{5}, \quad G_R = \frac{5C_{44}(C_{11} - C_{12})}{4C_{44} + (C_{11} - C_{12})}$$

III. 13

So:

$$G = \frac{G_R + G_H}{2}$$

III. 14

✓ Young's modulus

Young's modulus or modulus of elasticity (longitudinal) or tensile modulus is the constant that relates the tensile stress (or compression) and the deformation for an isotropic elastic material. It was the British physicist Thomas Young (1773-1829) who noticed that the ratio between the tensile stress applied to a material and the resulting deformation (a relative elongation) is constant, as long as this deformation remains small and the elastic limit of the material is not reached. In the case of a crystalline material, Young's modulus expresses the electrostatic "restoring force" that tends to keep the atoms at a constant distance. It is expressed in the following form:

$$E = \frac{9BG_H}{3B + G_H}$$

III. 15

✓ The Poisson coefficient

The Poisson coefficient is one of the elastic constants. It is between -1 and 0.5. Values experimental obtained in the case of a perfectly isotropic material are very close to the value (1/4). For any material, an average of 0.3 is obtained. There are also materials with a negative Poisson coefficient: this is sometimes referred to as auxetic materials. The fish coefficient is given in the following form:

$$\nu = \frac{3B - E}{6B}$$

III. 16

✓ **Anisotropic parameter:**

An isotropic medium is a medium whose properties are identical regardless of the direction of observation. For example, liquids or amorphous solids are (statistically) isotropic while crystals, whose structure are ordered and therefore depend on the direction, are anisotropic. Isotropy characterizes the invariance of the physical properties of a medium as a function of direction. The opposite of isotropy is anisotropy, which is the property of being dependent on direction. Its expression is given in the form:

$$A = \frac{2C_{44}}{C_{11} - C_{12}}$$

III. 17

✓ **Debye temperature and elastic wave velocities**

➤ **sound propagation velocity :**

In a solid, the velocity of mechanical waves is dependent on density ρ and elasticity constants. In the case of compression waves propagating without generating Transverse deformation it is the Young module E that comes into account. Three speeds of sound propagation are defined:

1) Speed of sound propagation (Longitudinal):

$$V_l = \left(\frac{3B + 4G}{3\rho} \right)^{\frac{1}{2}}$$

III. 18

Avec ρ : la masse volumique

2) Speed of sound propagation (Transversal) :

$$V_t = \left(\frac{G}{\rho} \right)^{\frac{1}{2}}$$

III. 19

3) Speed of its average:

$$V_m = \left[\frac{1}{3} \left(\frac{2}{V_t^3} + \frac{1}{V_l^3} \right) \right]^{\frac{1}{3}}$$

III. 20

After having determined the different mechanical quantities we can obtain the Debye temperature in the first place which is closely related to the physical quantities it is given by:

$$\theta_D = \frac{h}{k_B} \left[\frac{3}{4\pi} \left(\frac{N_A \rho}{M} \right) \right]^{\frac{1}{3}} V_m$$

III. 21

With N_A the Avogadro number; and M the molar mass

➤ **Full Heusler**

Table 12: gives the calculated values of the Mechanical properties for Co_2CrAl

Grandeurs Mécanique	Co_2CrAl
G(GPa)	87.657
B(GPa)	159.381
E(GPa)	222.231
ν	0.26
A	3.688
Vm(m/s)	3824.447
$\theta_D(K)$	502.469

➤ **Half Heusler**

Table 13: gives the calculated values of the Mechanical properties for $CoCrSb$

Grandeurs Mécanique	Co_2CrAl
G(GPa)	56.5532
B(GPa)	181.497
E(GPa)	153.6961
ν	0.3588
A	0.5961
Vm(m/s)	3010.537
$\theta_D(K)$	351.255

According to Table [12,13], the Poisson coefficient also provides information on the type of chemical bond, which is usually in the vicinity of **0.3588** for ionic materials and about 0.1 for covalent materials, which allows us to say that our compounds are ionic materials.

It is clear that the parameter Anisotropy A is close to unity for Co_2CrAl , $CrCoSb$ materials which allows us to say that these compounds are isotropic.

From the point of view of ductility and fragility, the B/G ratio for the four materials is generally above the critical value 3.21 which separates the ductile/fragile (fragile $< 1.75 <$ ductile) behaviors which allows us to classify the compounds as ductile material.

➤ **Elastic anisotropy**

The simplest way to illustrate the anisotropy of the polycrystalline bulk (B) and Young modulus (E) is to plot them in the two-dimensional surface (and/or three-dimensional) as a function of direction. We plotted the Young (E) and bulk modulus (B) in different directions using spherical coordinates for *full* (Co_2CrAl) and *half Heusler* ($CoCrSb$) compounds. For

cubic crystal class, the directional dependence of Young modulus E and bulk modulus B can be written as [25] :

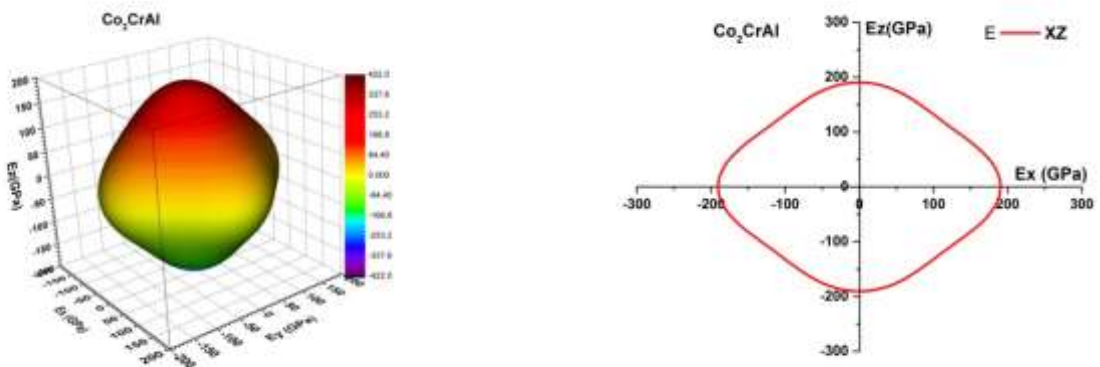
$$1/B = (S_{11} + S_{12})(l_1^2 + l_2^2 + l_3^2) \tag{III.22}$$

$$1/E = S_{11} + \left(S_{11} - S_{12} - \frac{1}{2}S_{44} \right) + (l_1^2 l_2^2 + l_2^2 l_3^2 + l_3^2 l_1^2) \tag{III.23}$$

In the equations above, S_{ij} represents the compliance matrix and l_1, l_2 and l_3 are the direction cosines, which are given as $l_1 = \sin\theta \cos\phi, l_2 = \sin\theta \sin\phi$ and $l_3 = \cos\theta$ in the spherical coordinates.

For an isotropic system, 2D directional dependence would give rise to a circle shape, while the deviation degree from circle shape reflects the degree of anisotropy.

The projections on (XY) and (XZ) planes of the bulk and Young’s modulus are shown in Fig4 From this figure, it is clear that along the X, Y and Z axis the compression is the same for all studied compounds due to the cubic system.



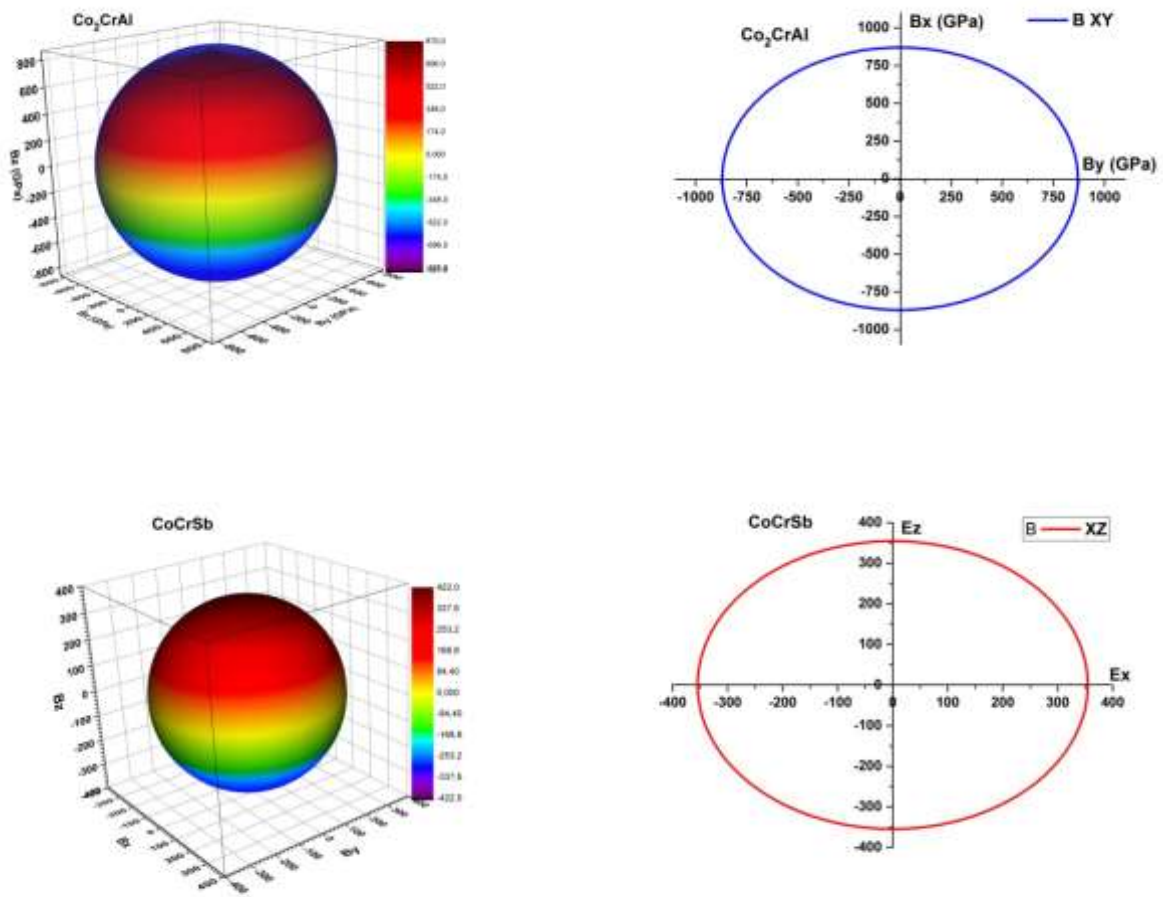


Figure 7: Anisotropy of Young's modulus and bulk's modules in Co₂CrAl and CoCrSb.

II.4.6 Thermodynamic properties

There are other useful and important thermodynamic parameters for understanding the behaviour of materials when used in a very high environment temperatures, such as melting temperature T_m , coefficient of thermal expansion and minimum thermal conductivity k_{min} .

The melting temperature T_m can give an idea of the atomic bond and the coefficient of thermal expansion of materials, a high melting temperature indicates a strong atomic bond and a low coefficient of thermal expansion. The melting temperature also makes it possible to determine the limits of materials used continuously in extreme conditions and in aggressive environments (oxidation, chemical transformations and excessive deformations) [26].

The melting temperature of cubic crystalline solids can be calculated from the elastic constant C_{11} using equation[26-28]:

$$T_m = 553 + 5.91 C_{11} \tag{III. 24}$$

Information on the minimum thermal conductivity (k_{min}) of a material is needed to control its applications at high temperatures. It is defined as the thermal conductivity of a material, which reaches its minimum value at a sufficiently high temperature [29]. At high temperatures, Clarke's formula[28] is used to calculate the minimum thermal conductivity k_{min} (W/mK) of materials:

$$k_{min} = k_B * v_m (V_{atomic})^{-2/3} \tag{III. 25}$$

Where, k_B is the Boltzmann constant, V_m is the average speed of sound and V_{atomic} is the volume cell by atom.

For the calculation of the coefficient of thermal expansion, the following formula was used[30]

$$\alpha = 1.6 \times 10^{-3} / G \tag{III. 26}$$

➤ **Full Heusler**

Table14: groups together the results of calculation of thermodynamic parameters for the compound Co2CrAl studied in this chapter.

	A	k_{min}	Tm
Co2CrAl	0.018.10⁻³	3.70*10 ⁻²⁵	2038.348

➤ **Half Heusler**

Table15: groups together the results of calculation of thermodynamic parameters for the compound CoCrSb studied in this chapter.

	A	k_{min}	Tm
CoCrSb	0.022.10⁻³	3.05*10 ⁻²⁵	2054.448

Reference

- [1]. Segall, M., et al., *First-principles simulation: ideas, illustrations and the CASTEP code*. Journal of Physics: Condensed Matter, 2002. **14**(11): p. 2717.
- [2]. Vanderbilt, D., *Soft self-consistent pseudopotentials in a generalized eigenvalue formalism*.
- [3]. Anglada, J.M. and J.M. Bofill, *How good is a Broyden–Fletcher–Goldfarb–Shanno-like update Hessian formula to locate transition structures? Specific reformulation of Broyden–Fletcher–Goldfarb–Shanno for optimizing saddle points*. Journal of computational chemistry, 1998. **19**(3): p. 349-362.
- [4]. Broyden, C.G., *The convergence of a class of double-rank minimization algorithms: 2. The new algorithm*. IMA journal of applied mathematics, 1970. **6**(3): p. 222-231.
- [5] Fletcher, R., *A new approach to variable metric algorithms*. The computer journal, 1970. **13**(3): p. 317-322.
- [6].Goldfarb, D., *A family of variable-metric methods derived by variational means*. Mathematics of computation, 1970. **24**(109): p. 23-26.
- [7].Shanno, D.F., *Conditioning of quasi-Newton methods for function minimization*. Mathematics of computation, 1970. **24**(111): p. 647-656. Physical Review B, 1990. **41**(11): p. 7892-7895.
- [8] Jen-Chuan Tung¹ and Guang-Yu Guo^{1,2,3}, Graduate Institute of Applied Physics, National Chengchi University, Taipei 11605, Taiwan (2013)
- [9] H. C. Kandpal, G. H. Fecher and C. Felser, J. Phys. D: Appl. Phys. 40, 1507 (2006).
- [10] D. P. RAI, A. SHANKAR, SANDEEP , M. P. GHIMIRE and R. K. THAPA India (2012)
- [11] Wyckoff, R.W.G. Crystal Structures, Crystal Structures, 2nd ed.; John Wiley and Sons: Hoboken, NJ, USA, 1963; Volume 1.
- [12] Kanpal, H.C.; Felse, C.; Seshadri, R. Covalent bonding and the nature of band gaps in some half-Heusler compounds. J. Phys. D Appl. Phys. **2006**, 39, 776.
- [13] Nanda, B.R.K.; Dasgupta, J.I. Electronic structure and magnetism in half-Heusler compounds. Phys. Condens. Matter **2003**, 15, 73077323.
- [14] Jen-Chuan Tung¹ and Guang-Yu Guo^{1,2,3}, Graduate Institute of Applied Physics, National Chengchi University, Taipei 11605, Taiwan (2013).

- [15] D. P. RAI, A. SHANKAR, SANDEEP , M. P. GHIMIRE and R. K. THAPA India (2012).
- [16] Zhong-Yu, Y.; Li, S.; Meng-Mei, P.; Shu-Juan, S. First-principle studies of half-metallicities and magnetisms of the semi-Heusler alloys CoCrTe and CoCrSb. *Acta Phys. Sin.* **2016**, 65, 127501.
- [17] Zhong-Yu, Y.; Li, S.; Meng-Mei, P.; Shu-Juan, S. First-principle studies of half-metallicities and magnetisms of the semi-Heusler alloys CoCrTe and CoCrSb. *Acta Phys. Sin.* **2016**, 65, 127501.
- [18] D P Rai^{1*}, A Shankar¹, Sandeep¹, M P Ghimire² and R K Thapa¹. *Journal of Theoretical and Applied Physics* (2013).
- [19] D. P. RAI, A. SHANKAR, SANDEEP , M. P. GHIMIRE and R. K. THAPA India (2012)
- [20] Slater, J., *JC Slater, Phys. Rev. 49, 537 (1936)*. *Phys. Rev.*, 1936. **49**: p. 537.
- [21]. Pauling, L., *L. Pauling, Phys. Rev. 54, 899 (1938)*. *Phys. Rev.*, 1938. **54**: p. 899.
- [22] Zhong-Yu, Y.; Li, S.; Meng-Mei, P.; Shu-Juan, S. First-principle studies of half-metallicities and magnetisms of the semi-Heusler alloys CoCrTe and CoCrSb. *Acta Phys. Sin.* **2016**, 65, 127501.
- [23] M. J. Mehl, *Phys. Rev. B*47, 2493(1993).
- [24] Born Max, Huang Kun, dynamical theory of crystal lattices (paper) (reissue 1998).
- [25] J. F. Nye, *Physical properties of crystals: their representation by tensors and matrices*: Oxford university press, 1985.

General *Conclusion*

Conclusion générale :

We applied the PP-LAPW method with the GGA approach to study the physical properties and more particularly the structural, elastic, electronic, and magnetic properties of the Heusler Co_2CrAl and CoCrSb compound. In order to identify the qualities of this material that can inform about the possibility of being a good candidate for spintronic applications.

According to our calculation, the results obtained are as follows:

➤ **Structural properties:**

The most important step is to determine the structural properties of a given system in its ground state. The ternary Heusler alloy (Co_2CrAl can have full regular and CoCrSb can have three different types of structures).

According to the case calculations, our compound is stable in the type-II ferromagnetic phase, which makes it possible to determine the corresponding equilibrium parameters such as the lattice constant a , the volume V_0 , minimum energy.

➤ **Elastic properties:**

The elastic constants obtained from the calculation of the elastic properties indicate the mechanical stability of our compound. The anisotropic parameter A is different from unity for what allows us to say that it is anisotropic. From the point of view of ductility and fragility, the B/G ratio is greater than the critical value 1.75 which separates ductile / fragile behavior ($\text{fragile} < 1.75 < \text{ductile}$), so we can classify our compound as a ductile material.

➤ **Electronic and magnetic properties:**

From the calculation of the electronic band structure and the spin-polarized total density of states (DOS), we found the presence of the indirect gap in the minority spin. Moreover, from the magnetic properties, we calculated the total magnetic moment of Co_2CrAl and CoCrSb as well as the magnetic moment of each atom. We can say that the presence of Co increases the total magnetic moment, the spin polarization is 100% in addition the Slater-Pauling rules $Mt=27-24=3\mu_B$ and $Mt=20-18=2\mu_B$ is verified. All these properties allow us to say that the alloy to a half-metallic character.

➤ **Thermodynamic properties**

Information on the minimum thermal conductivity (k_{\min}) of a material is needed to control its applications at high temperatures. It is defined as the thermal conductivity of a material, which reaches its minimum value at a sufficiently high temperature

البحث عن مواد جديدة ذات خصائص محددة للإلكترونيات السبينية

الغرض هو اقتراح المواد التي تلي الاحتياجات الصناعية. لهذا السبب نحن مهتمون بهذا العمل لدراسة عائلة من المواد الذكية وهي سبائك Heusler ، وقد ثبت أن هذه الفئة من المواد قادرة على التغلب على هذه التحديات كمرشحين محتملين بخصائص مثيرة للاهتمام للإلكترونيات السبينية . تم تخصيص هذا العمل النظري لدراسة سبائك Heusler. وضعنا أنفسنا في إطار نظرية الكثافة الوظيفية باستخدام طرق ab initio المطبقة في حزمة Castep لدراسة الخصائص المغناطيسية الإلكترونية والكيميائية والميكانيكية. درسنا Heusler الكامل كمادة نصف معدنية تمتلك درجة حرارة عالية واستقطاب Fermi الكلي بالإضافة إلى عزم مغناطيسي كبير. لقد طورنا أيضًا تصحيحًا ملحوظًا لفجوات الطاقة بطريقة GGA. بعد ذلك ، اقترحنا مرحلة تكعيبية جديدة لسبائك هوسلر النصفية تتميز بعزم مغناطيسي كبير بالإضافة إلى درجة حرارة كوري عالية وتكون ذات صلة بالتطبيقات المستقبلية. لقد اقترحنا عائلة جديدة من سبائك Heusler الثلاثية ذات الخصائص الرائعة على مستوى Fermi تسمى أشباه الموصلات المغزلية الجديدة الخالية من الفجوات. أخيرًا ، درسنا سبائك Heusler كمرشحين للناقلية الفائقة

الكلمة الرئيسية: سبنترونك ، أبتريو ، كاستيب ، سبائك هوسلر

Abstract

Research of new materials with specific properties for spintronics

The purpose being to propose materials that meet industrial needs . For this reason we are interested in this work to study a family of smart materials that are the Heusler alloys , this class of materials are shown to be able to overcome these challenges as potential candidates with interesting properties for spintronics. theoretical work is devoted to the study of Heusler alloys . We placed ourselves within the framework of the density functional theory using ab initio methods implemented in the Castep package to study the magneto - electronic, chemical and mechanical properties . We studied the full Heusler as half metallic materials possessing high temperature , total Fermi polarization as well as a large magnetic moment . We have also developed a remarkable correction on energy gaps by the GGA method . Then , we proposed a new cubic phase of the half - Heusler alloys characterized by a large magnetic moment as well as a high Curie temperature and which is relevant for future applications. We have proposed a new family of ternary Heusler alloys with remarkable properties at Fermi level called new spin gapless semiconductors . Finally , we studied Heusler alloys as candidates for superconductivity .

Key Word : spintronic , ab initio , casteb , Heusler alloys

Résumé

Recherche de nouveaux matériaux avec des propriétés spécifiques pour la spintronique.

Le but étant de proposer des matériaux qui répondent aux besoins industriels. C'est pour cette raison que nous nous intéressons dans ce travail à l'étude d'une famille de matériaux intelligents qui sont les alliages de Heusler, cette classe de matériaux s'avère être capable de surmonter ces défis en tant que candidats potentiels avec des propriétés intéressantes pour la spintronique. Ce travail théorique est consacré à l'étude des alliages de Heusler . Nous nous sommes placés dans le cadre de la théorie de la fonctionnelle de la densité en utilisant des méthodes ab initio implémentées dans le package Castep pour étudier les propriétés magnéto - électroniques, chimiques et mécaniques. Nous avons étudié les Heusler complets comme des matériaux semi-métalliques possédant une température élevée, une polarisation de Fermi totale ainsi qu'un moment magnétique important. Nous avons également développé une correction remarquable sur les écarts d'énergie par la méthode GGA. Ensuite, nous avons proposé une nouvelle phase cubique des alliages de demi-Heusler caractérisée par un grand moment magnétique ainsi qu'une température de Curie élevée et qui est pertinente pour des applications futures. Nous avons proposé une nouvelle famille d'alliages ternaires de Heusler avec des propriétés remarquables au niveau de Fermi appelés nouveaux semi-conducteurs sans gap de spin . Enfin, nous avons étudié les alliages de Heusler comme candidats à la supraconductivité.

Mot clé : spintronique, ab initio, casteb, alliages de Heusler